Article | Received 15 April 2024; Accepted 16 July 2024; Published 6 August 2024
https://doi.org/10.55092/aias20240005

Cooperative adaptive fault-tolerant control for heterogeneous multiagent systems with guaranteed performance

Jianye Gong[1], Xiuli Wang[2], Yang Li[3,*] and Dandan Lyu[4]

[1]College of Electrical Engineering, Anhui Polytechnic University, Wuhu, China
[2]College of Information Engineering, Zhejiang University of Technology, Hangzhou, China
[3]School of Mechatronic Engineering and Automation, Shanghai University, Shanghai, China
[4]College of Computer Science and Technology, Zhejiang University, Hangzhou, China

* Correspondence author; E-mail: yongerli@shu.edu.cn.

Abstract: This paper studies the fault-tolerant control problem for the heterogeneous multiagent systems consisting of multiple quadrotors and mobile robots with guaranteed performance in the presence of unknown actuator faults. First, the full-state performance constraints of the position and attitude subsystem of follower vehicles are considered, especially in the case of actuator faults, and then the state constraints of heterogeneous unmanned systems are addressed by combining the performance functions and barrier Lyapunov function method. Then, the constraints-based cooperative adaptive fault-tolerant control strategy is proposed, where the adaptive terms are adopted to compensate for the unknown bounded actuator loss of effectiveness faults and bias faults and the constraint signals are introduced to ensure the performance conditions of system states. Based on the theoretical analysis, the cooperative fault-tolerant time-varying formation convergence performance is discussed. The simulation results on the UAVs-UGVs formation systems composed of quadrotors and mobile robots are presented to validate the effectiveness of the proposed control strategy.

Keywords: fault-tolerant control; adaptive control; heterogeneous miltiagent systems; actuator fault; performance constraint

1. Introduction

In recent years, there has been a growing interest in the cooperative formation control of multiagent systems (MASs) due to its wide range of practical applications. The formation tracking problem has become a focal point in research, aiming to design appropriate control strategies to track dynamic trajectories and maintain desired formation structures. This problem has been extensively studied across various domains, including collaborative search and rescue missions involving unmanned vehicles [1–3], formation flying of multiple satellites for astronomical and deep-space exploration [4–6]. Compared to homogeneous MASs, the cooperative control of heterogeneous MASs has greater challenges, which are not only from differences in system parameters but also from the heterogeneous state dimensions of dynamic systems.

The cooperative output regulation problem of heterogeneous MASs has garnered considerable attention recently. Unlike homogeneous MASs, state consensus schemes are not directly applicable to heterogeneous MASs. These systems consist of agents with different dynamic structures and physical parameters, making traditional state consensus approaches unsuitable. Consequently, researchers have increasingly focused on output regulation problems for heterogeneous MASs, as explored in [7], the output formation problem was investigated

for heterogeneous linear MASs, and a distributed output formation tracking protocol based on neighborhood interactions was proposed. However, the real physical systems usually contain nonlinear terms, such as heterogeneous MASs composed of multiple unmanned aerial vehicles (UAVs) and unmanned ground vehicles (UGVs), each with nonidentical physical models. Therefore, the control schemes for linear MASs cannot be directly applied to the UAVs-UGVs formation systems. Despite the challenges associated with controlling heterogeneous UAVs-UGVs formation systems, they find wide-ranging applications in various real-world scenarios. For instance, in speeding up forest fire rescue operations, a group of UAVs can monitor forest fires in real-time and provide rescue locations for ground-based UGVs, enabling swift execution of rescue missions. Consequently, recent attention has been directed towards the cooperative formation problem of the UAVs-UGVs colleborative systems. In [8], the observer-based fault-tolerant controller policies are designed for the team of heterogeneous vehicles via reinforcement learning. Additionally, [9] studied time-varying output formation problems for multiple UAVs-UGVs cooperative systems with switching directed topologies. Nonetheless, the cooperative formation control problem of the UAVs-UGVs system investigated in [8] and [9] are limited. The existence of nonidentical systems parameters and structures between UAVs and UGVs may significantly increase the difficulty of the control design, so it is important to study how to deal with the heterogeneous dynamic structures and further achieve the cooperative formation tracking more effectively.

In addition, considering the accuracy and safety factors in the formation process of MASs, the system states also havecertain limitations and constraints. If the system violates these restrictions, it may cause system performance degradation and even cause serious security problems. Therefore, investigating cooperative formation control with constraints is of great significance to ensure the safe operation of MASs [10–15].

In [10], the consensus control problem is studied for uncertain nonlinear multiagent systems with output constraint, and a distributed adaptive fuzzy output feedback control scheme based on barrier Lyapunov functions (BLFs) is proposed. In [11], the adaptive tracking control problem was considered for nonlinear multiagent systems under a directed graph and state constraints, and the integral barrier Lyapunov functionals are introduced to relax the feasibility conditions. [12] investigated the containment control for state-constrained MASs, and a log-type nonlinear state-dependent barrier function is established to cope with the time-varying asymmetric full-state constraints. In [13], the event-triggered consensus control is investigated for a category of uncertain nonlinear MASs with full-state constraints. The finite-time cooperative control and fixed-time control were developed for nonlinear MASs with full-state constraints in [14] and [15], respectively. The above mentioned works mainly concentrate on the study of constraint control for homogeneous MASs and do not consider the heterogeneous MASs which have different system structures. In [16], the cooperative control for heterogeneous MASs with time-varying full state constraints, and the nonlinear state-dependent function is introduced to construct the new systems, which is free of constraints. However, for such networked UAVs-UGVs systems with heterogeneous structures and uncertain system parameters, how to guarantee the performance constraints of system states is an important issue to be addressed.

In addition, these complex real-world systems are accompanied by various challenges such as actuator faults, which may seriously affect the performance and stability of the system. The occurrence of actuator faults, such as reduced propeller efficiency in a quadrotor or reduced drive wheel torque in a mobile robot, leads to uncertainty in the control gain matrix, which makes control design more difficult. In recent years, fault-tolerant control (FTC), has attracted widespread attention, which aims to design a control scheme that automatically compensates for faults and maintains system performance, and has been applied in various fields [17–20]. Fault-tolerant control methods are also combined with other technical methods to solve fault diagnosis and fault-tolerant control problems, such as robust control [21–23], artificial intelligence [24,25], and applications in aerospace [26–28]. With regard to multiple heterogeneous autonomous

unmanned systems, the fault-tolerant cooperative control problem was investigated in [29], and the FTC cooperative strategy is designed to re-coordinate the motion of each UAV and UGV in the whole team. To the best of our knowledge, although there have been many FTC studies on a single system or a class of homogeneous MASs, considering the comprehensive impact of the state constraints of UAVs and UGVs during the formation process, especially under the influence of unknown actuator faults, how to ensure system performance has become an interesting and challenging questions, which also motivated this study.

In this paper, we consider the UAVs-UGVs formation systems with actuator faults and full-state constraints. The main contributions of this paper are presented as follows:

1) A new cooperative fault-tolerant adaptive control scheme is developed, which can ensure system stability and fault-tolerant tracking property for the multi-input multi-output heterogeneous UAVs-UGVs formation systems with full-state constraints.

2) The performance constraints of state variables of quadrotor UAVs and mobile robot UGVs are considered, and barrier Lyapunov functions are introduced in virtual control signals and fault-tolerant control signals to guarantee the full-state constraints, especially under the influence of actuator faults.

3) The control-gain reconstruction based adaptive controllers are constructed to deal with the uncertain fault pattern matrix caused by actuator loss of effectiveness faults and bias faults.

The rest of this paper is arranged as follows: the preliminaries problem formulation are delivered in Section 2, while the main results of the designed constraint-based distributed adaptive fault-tolerant control scheme is elaborated in Section 3. Simulation study of the proposed control algorithm an the conclusion are presented in Section 4 and Section 5, respectively.

2. Preliminaries and problem formulation

In this section, the basic knowledge of graph theory is first presented, then, the dynamic models of the UAVs-UGVs formation systems are introduced, and the guaranteed-performance-based cooperative fault-tolerant problem for the UAVs-UGVs formation systems with actuator faults is formulated.

2.1. Graph theory

A directed interaction topology $\Xi \triangleq (\Sigma, \Phi, A)$ is presented to describe the information communication between $N+M$ unmanned systems, where $\Sigma \triangleq \{n_1, n_2, \ldots, n_{N+M}\}$ denotes the node set, $\Phi \subseteq \Sigma \times \Sigma$ denotes the edge set, and $A = [a_{kj}] \in R^{(N+M)\times(N+M)}$ represents the adjacency matrix. In the adjacency matrix A, the element a_{kj} represents the weight of the communication link and satisfies $a_{kj} > 0$ if $(n_k, n_j) \in \Phi$ and $a_{kj} > 0$ if $(n_k, n_j) \notin \Phi$. The edge $(n_k, n_j) \in \Phi$ implies that the node n_j can receive information from node n_k via a directed communication link, the set of neighbors of node n_k is $\mathscr{G}_k = \{j | (n_k, n_j) \in \Phi\}$. The Laplacian matrix L is expressed as $L = D - A$ with $D = \text{diag}\{d_{nk}\} \in R^{(N+M)\times(N+M)}$, where $d_{nk} = \sum_{j=1}^{N+M} a_{kj}$. Let b_{k0} represents the weight of the communication link between the leader vehicle and the kth follower agent, then the pinning matrix B is defined as $B = \text{diag}\{b_{k0}\} \in R^{(N+M)\times(N+M)}$.

2.2. Models of the UAVs-UGVs formation systems

In this paper, a group of heterogeneous multiagent systems including N quadrotors and M two-wheel driven mobile robots are considered. The dynamic modes of quadrotor UAVs and mobile robot UGVs are presented respectively.

Quadrotor model. The dynamics of the $k(k = 1, \ldots, N)$th quadrotor UAV can be formu-

lated as:

$$\begin{aligned}
\ddot{p}_{kx} &= (\cos\phi_k \sin\theta_k \cos\psi_k + \sin\psi_k \sin\phi_k)\frac{u_{kp}}{m_k} - \frac{\zeta_{kx}}{m_k}\dot{p}_{kx},\\
\ddot{p}_{ky} &= (\cos\phi_k \sin\theta_k \sin\psi_k + \cos\psi_k \sin\phi_k)\frac{u_{kp}}{m_k} - \frac{\zeta_{ky}}{m_k}\dot{p}_{ky},\\
\ddot{p}_{kz} &= (\cos\phi_k \sin\theta_k)\frac{u_{kp}}{m_k} - g - \frac{\zeta_{kz}}{m_k}\dot{p}_{kz},\\
\ddot{\phi}_k &= \frac{I_{ky}-I_{kz}}{I_{kx}}\dot{\theta}_k\dot{\psi}_k - \dot{\theta}_k\frac{J_{kr}}{I_{kx}}\Omega_{ka} - \frac{\zeta_{k\phi}}{I_{kx}}\dot{\phi}_k + \frac{u_{k\phi}}{I_{kx}},\\
\ddot{\theta}_k &= \frac{I_{kz}-I_{kx}}{I_{ky}}\dot{\psi}_k\dot{\phi}_k + \dot{\phi}_k\frac{J_{kr}}{I_{ky}}\Omega_{ka} - \frac{\zeta_{k\theta}}{I_{ky}}\dot{\theta}_k + \frac{u_{k\theta}}{I_{ky}},\\
\ddot{\psi}_k &= \frac{I_{kx}-I_{ky}}{I_{kz}}\dot{\phi}_k\dot{\theta}_k - \frac{\zeta_{k\psi}}{I_{kz}}\dot{\psi}_k + \frac{u_{k\psi}}{I_{kz}},
\end{aligned} \tag{1}$$

where $p_{ak} = [p_{kx}, p_{ky}, p_{kz}]^\top$ and $r_{ak} = [\phi_k, \theta_k, \psi_k]^\top$ represent the position variable and attitude variable of the kth quadrotor, respectively, m_k is the mass of the kth quadrotor, g is the acceleration of gravity, ζ_{kx}, ζ_{ky} and ζ_{kz} denote the aerodynamic damping coefficient, I_{kx}, I_{ky}, I_{kz} are the body inertia, J_{kr} and Ω_k denote the inertia and residual rotor angular, respectively, $\zeta_{k\varphi}, \zeta_{k\theta}, \zeta_{k\psi}$ are drag coefficients, u_{kp}, $u_{k\phi}$, $u_{k\theta}$ and $u_{k\psi}$ represent the control input generated by four rotors. All state variables are limited, which is described by $|p_{kl}| \le \bar{\chi}_{kl}, l = x, y, z$ and $|s_k| \le \bar{\chi}_{ks}, s = \phi, \theta, \psi$.

Two-wheel driven mobile robot model. The dynamics of the $k(k = 1, \ldots, M)$th mobile robot UGV is given as follows:

$$\begin{aligned}
\dot{p}_{kg} &= \begin{bmatrix} \cos\psi_k & 0 \\ \sin\psi_k & 0 \\ 0 & 1 \end{bmatrix} \begin{bmatrix} v_k \\ \omega_k \end{bmatrix},\\
M_k\dot{x}_{k\omega} &= -(D_k + C_k\dot{\psi}_k)x_{k\omega} + \tau_k,
\end{aligned} \tag{2}$$

where $p_{kg} = [p_{kx}, p_{ky}, \psi_k]^\top$ represents the position variables and the orientation variable of the kth UGV, v_k and ω_k are the linear and angular velocities, $x_{k\omega} = [\omega_{k1}, \omega_{k2}]^\top$ represents the angular velocities of the left and right wheels, $\tau_k = [\tau_{k1}, \tau_{k2}]^\top$ denotes the control torque, $D_k = \mathrm{diag}\{D_{k1}, D_{k2}\}$ denotes the surface friction, $C_k = \begin{bmatrix} C_{k1} & C_{k2} \end{bmatrix}$denotes the centripetal and coriolis matrix with $C_{k1} = [0, -c_k^*], C_{k2} = [c_k^*, 0]$, $c_k^* = 0.5h_k^{-1}r_k^2 m_{kc}c_{kg}$, and c_{kg} being the distance between the center of mass and the middle point of two wheels, $M_k = \begin{bmatrix} M_{k1} & M_{k2} \end{bmatrix}$ is the inertia matrix with $M_{k1} = [m_{k1}^*, m_{k2}^*]^\top$, $M_{k2} = [m_{k2}^*, m_{k1}^*]^\top$, $m_{k1}^* = \frac{1}{4h_k^2}r_k^2((m_{kc} + 2m_{k\omega})h_k^2 + I_{kg}) + I_{k\omega}$, $m_{k2}^* = \frac{1}{4h_k^2}r_k^2((m_{kc} + 2m_{k\omega})h_k^2 - I_{kg})$ and $I_{kg} = m_{kc}c_{kg}^2 + 2m_{k\omega}h_k^2 + I_{kc} + 2I_{km}$, and m_{kc} and $m_{k\omega}$ being the mass of the body and the wheel of the kth UGV, respectively, $I_{k\omega}$ being the moment of wheels with the motor about the wheel axis, I_{kc} and I_{km} being the moment of inertia of the kth vehicle about the vertical axis through the center of mass and the moment of wheels with the motor about the diameter, respectively. The position and orientation variables are limited, which satisfy $|p_{kl}| \le \bar{\chi}_{kl}, l = x, y$ and $|\psi_k| \le \bar{\chi}_{k\psi}$.

Since

$$\begin{bmatrix} v_k \\ \omega_k \end{bmatrix} = R_{hk}x_{k\omega}, \tag{3}$$

where $R_{hk} = \frac{r_k}{2}\begin{bmatrix} 1 & 1 \\ 1/h_k & -1/h_k \end{bmatrix}$ is a nonsingular matrix, r_k denotes the radius of the wheel

and h_k denotes the half width of the robot. From (3), define $\xi_k = [v_k, \omega_k]^\top$, we further have:

$$\dot{\xi}_k = -M_{Dk}\xi_k - M_{Ck}\omega_k\xi_k + M_{Rk}\tau_k, \tag{4}$$

where $M_{Rk} = (M_k R_{hk}^{-1})^{-1}$, $M_{Dk} = M_{Rk}D_k R_{hk}^{-1}$, $M_{Ck} = M_{Rk}C_k R_{hk}^{-1}$.

Then, to address the underactuated problem in the kinematic system model and facilitate the fault-tolerant control design, from [30], we introduce the coordinate transformation:

$$\begin{aligned} x_{kg} &= p_{kg} + \varphi_{k\mu}, \\ x_{k\psi} &= \psi_k + \varphi_{3k}, \end{aligned} \tag{5}$$

where $x_{kg} = [\bar{p}_{kx}, \bar{p}_{ky}]^\top$ and $x_{k\psi}$ are the transformed position and heading angle variables of the kth UGV, $p_{kg} = [p_{kx}, p_{ky}]^\top$, $\varphi_{k\mu} = [\varphi_{k\mu 1}, \varphi_{k\mu 2}]^\top$ with $\varphi_{k\mu 1} = \varphi_{1k}\cos x_{k\psi} - \varphi_{2k}\sin x_{k\psi}$ and $\varphi_{k\mu 2} = \varphi_{1k}\sin x_{k\psi} + \varphi_{2k}\cos x_{k\psi}$, $\varphi_{3k} = \upsilon_b \cos\mu_k$, $\varphi_{1k} = \upsilon_a \sin\mu_k \frac{\sin\varphi_3}{\varphi_3}$, $\varphi_{2k} = \upsilon_a \sin\mu_k \frac{1-\cos\varphi_3}{\varphi_3}$, $\upsilon_a > 0$ and $\upsilon_b \in (0, \pi/2)$ are positive parameters.

Then, the transformed kinematic system dynamics can be further obtained:

$$\begin{aligned} \dot{x}_{kg} &= \left[\begin{pmatrix} \cos\psi_k \\ \sin\psi_k \end{pmatrix} \quad \Xi_k \begin{pmatrix} \frac{\partial\varphi_{1k}}{\partial\mu_k} \\ \frac{\partial\varphi_{2k}}{\partial\mu_k} \end{pmatrix} \right] \begin{bmatrix} v_k \\ \dot{\mu}_k \end{bmatrix} + \frac{\partial\Xi_k}{\partial x_{k\psi}} \begin{bmatrix} \varphi_{1k} \\ \varphi_{2k} \end{bmatrix} \dot{x}_{k\psi}, \\ &= \Xi_{k\varphi} \begin{bmatrix} v_k \\ \dot{\mu}_k \end{bmatrix} + \frac{\partial\Xi_k}{\partial x_{k\psi}} \bar{\varphi}_k \dot{x}_{k\psi} \\ \dot{x}_{k\psi} &= \omega_k - \frac{\partial\varphi_{3k}}{\partial\mu_k}\dot{\mu}_k, \end{aligned} \tag{6}$$

where $\Xi_k = \begin{bmatrix} \Xi_{1k} & \Xi_{2k} \end{bmatrix}$, $\Xi_{1k} = [\cos x_{k\psi}, \sin x_{k\psi}]^\top$, $\Xi_{2k} = [-\sin x_{k\psi}, \cos x_{k\psi}]^\top$, $\bar{\varphi}_k = [\varphi_{1k}, \varphi_{2k}]^\top$, $\Xi_{k\varphi} = \begin{bmatrix} \Xi_{k\psi} & \Xi_{k\mu} \end{bmatrix}$, $\Xi_{k\psi} = [\cos\psi_k, \sin\psi_k]^\top$, $\Xi_{k\mu} = \Xi_k[\frac{\partial\varphi_{1k}}{\partial\mu_k}, \frac{\partial\varphi_{2k}}{\partial\mu_k}]^\top$. From (6), the kinematic system model in (2) is transformed into a nonlinear system with strict-feedback form, which is adopted in the following fault-tolerant control design.

Virtual leader model. The system dynamics of the virtual leader are given in the following form:

$$\dot{x}_0 = f_0(x_0, t), \tag{7}$$

where $x_{01} = [x_{0x}, x_{0y}]^\top \in R^2$ denotes the position coordinate of the virtual leader, $f_0(x_0, t) = [f_{0x}, f_{0y}]^\top$ represents the smooth function.

Assumption 1. The leader's state variable x_0 is bounded and continuous i.e., $|x_{0x}(t)| \le M_{0x}$ and $|x_{0y}(t)| \le M_{0y}$, where M_{0x} and M_{0y} are positive constants.

Actuator faults. In the UAVs-UGVs collaborative formation systems, the propellers of UAVs and the driving wheels of UGVs will suffer from certain faults inevitably due to the complex structures of heterogeneous MASs and flexible task scenarios. Consider the following actuator fault model:

$$u_{kif} = \sigma_{ki}u_{ki} + f_{uki}(t), k = 1, \ldots, N, i = p, \phi, \theta, \psi, \tag{8}$$

where u_{kif} is the actual control input of the kth quadrotor, $\sigma_{ki} \in (0, 1]$ and $f_{uki}(t) \in R$ denote the unknown loss of effectiveness fault and bias fault, respectively.

For the two-wheeled driven mobile robots, the control torque faults are modeled as:

$$\tau_{kf} = \sigma_k\tau_k + f_{\tau k}(t), k = 1, \ldots M, \tag{9}$$

where τ_{kf} is the actual control torque of the kth mobile robot, $\sigma_k = \mathrm{diag}\{\sigma_{k1}, \sigma_{k2}\}$ is fault pattern matrix with the fault factor $\sigma_{kl} \in (0, 1]$ for $l = 1, 2$, and $f_{\tau k}(t) = [f_{\tau k1}(t), f_{\tau k2}(t)]^\top$ denotes the vector of fault values.

Assumption 2. The bias fault values are bounded, i.e., $|f_{uki}(t)| \leq \bar{f}_{uki}$ for $k = 1,\ldots,N$, and $||f_{\tau k}(t)|| \leq \bar{f}_{\tau k}$ for $k = 1,\ldots M$, where $\bar{f}_{uki}$ and $\bar{f}_{\tau k}$ are unknown positive constants.

Remark 1: As pointed out in [20], Assumption 1 is a standard condition in leader-following control design. Since the dynamic trajectory of the leader is commonly regarded as the desired tracking path for each follower, it should be bounded in practice. As stated in [17], Assumption 2 is reasonable in dealing with the adaptive fault-tolerant control problem of actuator faults.

The UAVs-UGVs formation system model. The UAVs-UGVs formation systems considered in this paper is a typical class of heterogeneous MASs, and the system state structures and physical parameters are non-identical. In the following fault-tolerant control strategy, the UAVs-UGVs formation systems model is divided into the position subsystem and attitude subsystem, where the position subsystem includes the trajectory dynamic of the UAVs-UGVs system, and the attitude subsystem includes the attitude dynamics of UAVs.

Based on the above descriptions on system dynamic models and fault models, define the following agent sets $\mathscr{F}_a = \{1,\ldots,N\}$, $\mathscr{F}_g = \{1,\ldots,M\}$ and $\mathscr{F}_{ag} = \{1,\ldots,N+M\}$, thus, the position subsystem dynamic models of the $k, k \in \mathscr{F}_{ag}$th vehicle under faulty case can be expressed in the following form:

$$\begin{aligned} \dot{x}_{k1} &= F_{k1} + G_{k1}x_{k2}, \\ \dot{x}_{k2} &= F_{k2} + G_{k2}\Gamma_k u_k,\ k \in \mathscr{F}_{ag}, \end{aligned} \tag{10}$$

where $x_{k1} = [p_{kx}, p_{ky}, p_{kz}]^\top$, $F_{k1} = [0,0,0]^\top$, $G_{k1} = \mathrm{diag}\{1,1,1\}$, $x_{k2} = [\dot{p}_{kx}, \dot{p}_{ky}, \dot{p}_{kz}]^\top$, $F_{k2} = -\zeta_{km}\dot{x}_{k1} + f_{ukp}\Theta_k/m_k + g_a$, $g_a = [0,0,-g]^\top$, $\zeta_{km} = \mathrm{diag}\{\frac{\zeta_{kx}}{m_k}, \frac{\zeta_{ky}}{m_k}, \frac{\zeta_{kz}}{m_k}\}$, $G_{k2} = 1/m_k$, $\Gamma_k = \sigma_{kp}$, $u_k = u_{ka} = \Theta_k u_{kp}$ denotes the control channel of the quadrotor position system for $k \in \mathscr{F}_a$, $\Theta_k = [\cos\phi_k \sin\theta_k \cos\psi_k + \sin\psi_k \sin\phi_k, \cos\phi_k \sin\theta_k \sin\psi_k + \cos\psi_k \sin\phi_k, \cos\phi_k \sin\theta_k]^\top$; $x_{k1} = [x_{kg}^\top, x_{k\psi}]^\top$, $F_{k1} = [F_{k1p}^\top, F_{k1\psi}]^\top$, $F_{k1p} = \frac{\partial \Xi_k}{\partial x_{k\psi}}\bar{\varphi}_k\dot{x}_{k\psi}$, $F_{k1\psi} = -\frac{\partial \varphi_{3k}}{\partial \mu_k}\dot{\mu}_k$, $G_{k1} = \mathrm{diag}\{\Xi_{k\varphi}, 1\}$, $x_{k2} = [v_k, \dot{\mu}_k, \omega_k]^\top$, $F_{k2} = [F_{k2v}, \dot{\mu}_k, F_{k2\omega}]^\top$ with $F_{k2\tau} = [F_{k2v}, F_{k2\omega}]^\top = -M_{Dk}\xi_k - M_{Ck}\omega_k\xi_k + M_{Rk}f_{\tau k}$, $G_{k2} = \iota^\top M_{Rk}\iota$, $\iota = \begin{bmatrix} 1 & 0 & 0 \\ 0 & 0 & 1 \end{bmatrix}$, $\Gamma_k = \mathrm{diag}\{\sigma_{k1}, 0, \sigma_{k2}\}$, $u_k = [\tau_{k1}, 0, \tau_{k2}]^\top$ denotes the control torque of the mobile robot system for $k \in \mathscr{F}_g$.

Then, the attitude subsystem dynamic models of the kth quadrotor under faulty case can be expressed as:

$$\begin{aligned} \dot{x}_{kr} &= x_{k\omega}, \\ \dot{x}_{k\omega} &= F_{k\omega} + G_{k\omega}\Gamma_{k\omega}u_{k\omega},\ k \in \mathscr{F}_a, \end{aligned} \tag{11}$$

where $x_{kr} = r_{ak} = [\phi_k, \theta_k, \psi_k]^\top$, $x_{k\omega} = [\dot{\phi}_k, \dot{\theta}_k, \dot{\psi}_k]^\top$, $F_{k\omega} = [F_{k\omega}^\phi, F_{k\omega}^\theta, F_{k\omega}^\psi]^\top$, $F_{k\omega}^\phi = \frac{I_{ky}-I_{kz}}{I_{kx}}\dot{\theta}_k\dot{\psi}_k - \dot{\theta}_k\frac{J_{kr}}{I_{kx}}\Omega_{ka} - \frac{\zeta_{k\phi}}{I_{kx}}\dot{\phi}_k + \frac{f_{uk\phi}}{I_{kx}}$, $F_{k\omega}^\theta = \frac{I_{kz}-I_{kx}}{I_{ky}}\dot{\psi}_k\dot{\phi}_k + \dot{\phi}_k\frac{J_{kr}}{I_{ky}}\Omega_{ka} - \frac{\zeta_{k\theta}}{I_{ky}}\dot{\theta}_k + \frac{f_{uk\theta}}{I_{kx}}$, $F_{k\omega}^\psi = \frac{I_{kx}-I_{ky}}{I_{kz}}\dot{\phi}_k\dot{\theta}_k - \frac{\zeta_{k\psi}}{I_{kz}}\dot{\psi}_k + \frac{f_{uk\psi}}{I_{kz}}$, $G_{k\omega} = \mathrm{diag}\{1/I_{kx}, 1/I_{ky}, 1/I_{kz}\}$, $\Gamma_{k\omega} = \mathrm{diag}\{\sigma_{k\phi}, \sigma_{k\theta}, \sigma_{k\psi}\}$, $u_{k\omega} = [u_{k\phi}, u_{k\theta}, u_{k\psi}]^\top$ denotes the control signal of the attitude system of the follower quadrotor for $k \in \mathscr{F}_a$.

2.3. Control objective

For the UAVs-UGVs formation systems with guaranteed performance and actuator faults considered in this paper, the main objective is to develop adaptive fault-tolerant controllers such that:

1) the follower UAVs and UGVs can track the dynamic trajectory of the virtual leader and further obtain the expected time-varying formation configuration under the influence of actuator faults;

2) all signal in the UAVs-UGVs formation systems are bounded, and all state variables stay within constrained performance boundaries.

3. Constraint-based distributed adaptive fault-tolerant control scheme

In this section, the formation tracking errors of the UAVs-UGVs formation systems are first defined, then, a constraint-based distributed fault-tolerant control algorithm is proposed for the position subsystem of the UAVs-UGVs formation systems to obtain the desired time-varying formation configuration and full states performance constraints. The fault-tolerant adaptive cooperative control strategy is further developed for the attitude subsystem of follower UAVs to guarantee that the attitude angles can achieve consensus and maintain constraints.

3.1. Formation tracking errors

To facilitate the following fault-tolerant controller design, the formation tracking errors of the UAVs-UGVs formation systems are introduced as:

$$\begin{aligned} e_{kp} &= \sum_{j\in\mathscr{G}_j} a_{kj}((x_{kp}-\gamma_k)-(x_{jp}-\gamma_j))+b_{k0}(x_{kp}-\gamma_k-x_0), k\in\mathscr{F}_{ag},\\ e_{kz} &= p_{kz}-x_{0z}, k\in\mathscr{F}_a,\ e_{k\psi}=x_{k\psi}-x_{0\psi}, k\in\mathscr{F}_g,\\ e_{kr} &= x_{kr}-x_{0r}, k=\mathscr{F}_a, \end{aligned} \tag{12}$$

where $e_{kp}=[e_{kpx},e_{kpy}]^\top$ represents the neighborhood trajectory tracking error of follower UAVs and UGVs in the horizontal plane, $x_{kp}=[p_{kx},p_{ky}]^\top$ for $k\in\mathscr{F}_a$ and $x_{kp}=x_{kg}$ for $k\in\mathscr{F}_g$ denote the state variables in the forward and longitudinal directions, $\gamma_k=[\gamma_{kx},\gamma_{ky}]^\top$ is the desired formation structure vector, x_0 denotes the state information of the virtual leader; e_{kz} and $e_{k\psi}$ denote the altitude tracking error and the orientation tracking error of the kth follower UAV and UGV, respectively, x_{0z} is the desired flight altitude, $x_{0\psi}=\arctan(\dot{x}_{0y}/\dot{x}_{0x})$ denotes the desired heading angle; e_{kr} is the attitude tracking error of the follower UAV, $x_{0r}=[\phi_{kd},\theta_{kd},x_{0\psi}]^\top$ is the desired attitude information.

3.2. Fault-tolerant controller design for position subsystem of the UAVs-UGVs formation systems

The adaptive FTC scheme with state constraints for position subsystems is composed of the kinematic control laws design and the dynamic control laws design.

Kinematic control laws design. From (10) and (12), the dynamics of the error variables can be obtained as:

$$\begin{aligned} \dot{e}_{kp} &= (d_{nk}+b_{k0})(F_{k1p}+G_{k1p}x_{kv}-\dot{\gamma}_k)\\ &\quad -\sum_{j\in\mathscr{G}_j} a_{kj}(F_{j1p}+G_{j1p}x_{jv}-\dot{\gamma}_j)-b_{k0}\dot{x}_0,\ k\in\mathscr{F}_{ag},\\ \dot{e}_{kz} &= v_{kz}-\dot{x}_{0z},\ k\in\mathscr{F}_a, \dot{e}_{k\psi}=\omega_k-\frac{\partial\varphi_{3k}}{\partial\mu_k}\dot{\mu}_k-\dot{x}_{0\psi},\ k\in\mathscr{F}_g, \end{aligned} \tag{13}$$

where $F_{k1p}=[0,0]^\top$, $G_{k1p}=\mathrm{diag}\{1,1\}$, $x_{kv}=[\dot{p}_{kx},\dot{p}_{ky}]^\top$ for $k\in\mathscr{F}_a$, $F_{k1p}=\frac{\partial\Xi_k}{\partial x_{k\psi}}\bar{\varphi}_k\dot{x}_{k\psi}$, $G_{k1p}=\Xi_{k\varphi}$, $x_{kv}=[v_k,\dot{\mu}_k]^\top$ for $k\in\mathscr{F}_g$.

In the kinematic control design of the positon subsystem, the radial basis function neural network is employed to cope with the system unknown functions. The unknown nonlinear function $h(\varsigma)$ to be approximated can be expressed as:

$$h(\varsigma)=\vartheta^{*\top}\varpi(\varsigma)+\delta(\varsigma), \tag{14}$$

where $\varsigma=[\varsigma_1,\ldots,\varsigma_m]^\top\in R^m$ is the input signal of the neural network, $\vartheta^*=[\vartheta_1,\ldots,\vartheta_n]^\top$ represents ideal weight vectors, The basis function $\varpi(\varsigma)=[\varpi_1(\varsigma),\ldots,\varpi_n(\varsigma)]^\top\in R^n$ satisfies

$\varpi_i(\varsigma) = \exp(-\frac{(\varsigma-\Upsilon_i)^\top(\varsigma-\Upsilon_i)}{d_i^2})$, $i = 1,\ldots,n$ with $\Upsilon_i \in R^p$ and $d_i > 0$ being the center and width of $\varpi(\varsigma)$, $\delta(\varsigma)$ is the bounded optimal approximation error which satisfies $|\delta(\varsigma)| \leq \bar{\sigma}$ with $\bar{\varepsilon} > 0$ being a constant. Thus, from (13) and (14), the radial basis function neural network is constructed to approximate unknown functions in e_{kp} and the dynamics of e_{kp} can be rewritten as:

$$\begin{aligned} \dot{e}_{kp} &= (d_{nk} + b_{k0})G_{k1p}x_{kv} + h_{kp}, \\ &= (d_{nk} + b_{k0})G_{k1p}x_{kv} + \vartheta_{kp}^{*\top}\varpi_{kp}(\varsigma) + \delta_{kp}(\varsigma), \end{aligned} \tag{15}$$

where $h_{kp} = [h_{kpx}(\varsigma), h_{kpy}(\varsigma)]^\top = (d_{nk} + b_{k0})(F_{k1p} - \dot{\gamma}_k) - \sum_{j\in\mathscr{G}_j} a_{kj}(F_{j1p} + G_{j1p}x_{jv} - \dot{\gamma}_j) - b_{k0}\dot{x}_0$, $\varpi_{kp}(\varsigma) = [\varpi_{kpx}^\top(\varsigma), \varpi_{kpy}^\top(\varsigma)]^\top$, $\vartheta_{kp}^{*\top} = \mathrm{diag}\{\vartheta_{kpx}^{*\top}, \vartheta_{kpy}^{*\top}\}$ and $\sigma_{kp}(\varsigma) = [\sigma_{kpx}(\varsigma), \sigma_{kpy}(\varsigma)]^\top$ satisfy $||\vartheta_{kpl}^{*\top}|| \leq \bar{\vartheta}_{kpl}$ and $||\delta_{kpl}(\varsigma)|| \leq \bar{\delta}_{kpl}, l = x, y$ with $\bar{\vartheta}_{kpl}$ and $\bar{\delta}_{kpl}$ being unknown positive constants, $||\cdot||_F$ is the Frobenius norm.

Define the virtual error variables as $e_{k2} = x_{kv} - \alpha_{kp}$, $z_{kz} = \dot{p}_{kz} - \alpha_{kaz}$, $k \in \mathscr{F}_a$, where α_{kp} and α_{kaz} represent the virtual control signals. Then, the virtual control law $\alpha_{ka} = [\alpha_{kp}^\top, \alpha_{kaz}]^\top$ for the kth follower quadrotor UAV is designed as:

$$\alpha_{ka} = \begin{bmatrix} \frac{1}{d_{nk}+b_{k0}}(-k_1 e_{kp} - \Xi_{k\varpi}\hat{\vartheta}_{kp} - \frac{1}{2}z_{\eta k}) \\ -k_{az}e_{kz} + \dot{x}_{0z} \end{bmatrix}, k \in \mathscr{F}_a, \tag{16}$$

further, let the error variables $z_{kv} = v_k - \alpha_{kv}$, $z_{k\omega} = \omega_k - \alpha_{k\omega}$, $k \in \mathscr{F}_g$, α_{kv} and $\alpha_{k\omega}$ represent the virtual control signals, the virtual control law $\alpha_{kg} = [\alpha_{kp}^\top, \alpha_{k\psi}]^\top$ with $\alpha_{kp} = [\alpha_{kv}, \dot{\mu}_k]^\top$ for the kth follower mobile robot UGV is designed as:

$$\alpha_{kg} = \begin{bmatrix} \Xi_{k\varphi}^{-1}\left(\frac{1}{d_{nk}+b_{k0}}(-k_1 e_{kp} - \Xi_{k\varpi}\hat{\vartheta}_{kp} - \frac{1}{2}z_{\eta k}) - \frac{\partial \Xi_k}{\partial x_{k\psi}}\bar{\varphi}_k(k_{g\psi}e_{k\psi} - \dot{x}_{0\psi})\right) \\ -k_{g\psi}e_{k\psi} + \frac{\partial \varphi_{3k}}{\partial \mu_k}\dot{\mu}_k + \dot{x}_{0\psi} \end{bmatrix}, k \in \mathscr{F}_g, \tag{17}$$

where $z_{\eta k} = [z_{\eta kx}, z_{\eta ky}]^\top$ with $z_{\eta kx} = \frac{e_{kpx}}{\eta_{kx}^2 - e_{kpx}^2}$ and $z_{\eta ky} = \frac{e_{kpy}}{\eta_{ky}^2 - e_{kpy}^2}$, $|e_{kpx}| < \eta_{kx}$ and $|e_{kpy}| < \eta_{ky}$, $\eta_{kx} > 0$ and $\eta_{ky} > 0$ denote the constraint values, $\Xi_{k\varpi} = \mathrm{diag}\{\frac{z_{\eta kx}||\varpi_{kpx}||_F^2}{2\kappa_{kpx}^2}, \frac{z_{\eta ky}||\varpi_{kpy}||_F^2}{2\kappa_{kpy}^2}\}$, $\kappa_{kpx} > 0$ and $\kappa_{kpy} > 0$ are designed constants, $\hat{\vartheta}_{kp} = [\hat{\vartheta}_{kpx}, \hat{\vartheta}_{kpy}]^\top$ is the estimate of $\bar{\vartheta}_{kp} = [\bar{\vartheta}_{kpx}, \bar{\vartheta}_{kpy}]^\top$, $k_1 > 0$, $k_{az} > 0$ and $k_{g\psi}$ are designed parameters.

To update the virtual control signal α_{ka}, we construct the adaptive law $\dot{\hat{\vartheta}}_{kp}$ as:

$$\dot{\hat{\vartheta}}_{kp} = \lambda_{kp}\Xi_{k\varpi}z_{\eta k} - \varepsilon_{kp}\hat{\vartheta}_{kp}, k \in \mathscr{F}_a, \tag{18}$$

where $\lambda_{kp} > 0$ and $\varepsilon_{kp} > 0$ are designed positive parameters.

Consider a positive candidate function V_{p1} to perform a preliminary analysis of α_{ka} and α_{kg} as:

$$\begin{aligned} V_{p1} = &\sum_{k\in\mathscr{F}_{ag}} \frac{1}{2}(\log\frac{\eta_{kx}^2}{\eta_{kx}^2 - e_{kpx}^2} + \log\frac{\eta_{ky}^2}{\eta_{ky}^2 - e_{kpy}^2}) + \sum_{k\in\mathscr{F}_{ag}} \frac{1}{2\lambda_{kp}}\tilde{\vartheta}_{kp}^\top\tilde{\vartheta}_{kp} \\ &+ \sum_{k\in\mathscr{F}_a} \frac{1}{2}\log\frac{\eta_{kz}^2}{\eta_{kz}^2 - e_{kz}^2} + \sum_{k\in\mathscr{F}_g} \frac{1}{2}\log\frac{\eta_{k\psi}^2}{\eta_{k\psi}^2 - e_{k\psi}^2}, \end{aligned} \tag{19}$$

where $\tilde{\vartheta}_{kp} = \bar{\vartheta}_{kp} - \hat{\vartheta}_{kp}$ is the estimation error, e_{kz} and $e_{k\psi}$ satisfy $|e_{kz}| < \eta_{kz}$ and $e_{k\psi} < \eta_{k\psi}$, η_{kz} and $\eta_{k\psi}$ denote the constraint values of the altitude tracking error of follower UAVs and the orientation tracking error of follower UGVs, respectively.

On the basis of the dynamic functions in (13), the derivative of V_{p1} is

$$\dot{V}_{p1} = \sum_{k\in\mathscr{F}_{ag}} z_{\eta k}^{\top}((d_{nk}+b_{k0})G_{k1p}x_{kv} + \vartheta_{kp}^{*\top}\varpi_{kp}(\varsigma)+\sigma_{kp}(\varsigma)) + \sum_{k\in\mathscr{F}_a}\frac{e_{kz}}{\eta_{kz}^2-e_{kz}^2}(v_{kz}-\dot{x}_{0z})$$
$$+\sum_{k\in\mathscr{F}_g}\frac{e_{k\psi}}{\eta_{k\psi}^2-e_{k\psi}^2}(\omega_k-\frac{\partial\varphi_{3k}}{\partial\mu_k}\dot{\mu}_k-\dot{x}_{0\psi}) - \sum_{k\in\mathscr{F}_{ag}}\frac{1}{\lambda_{kp}}\tilde{\vartheta}_{kp}^{\top}\dot{\hat{\vartheta}}_{kp}. \tag{20}$$

Then, by utilizing Young's inequality, one can obtain that:

$$z_{\eta k}^{\top}\vartheta_{kp}^{*\top}\varpi_{kp}(\varsigma) \le z_{\eta k}^{\top}\Xi_{k\varpi}\bar{\vartheta}_{kp} + \frac{1}{2}(\kappa_{kpx}^2+\kappa_{kpy}^2), \tag{21}$$
$$z_{\eta k}^{\top}\delta_{kp}(\varsigma) \le \frac{1}{2}z_{\eta k}^{\top}z_{\eta k} + \frac{1}{2}(\bar{\delta}_{kpx}^2+\bar{\delta}_{kpy}^2), \tag{22}$$

where $\Xi_{k\varpi} = \mathrm{diag}\{\frac{z_{\eta kx}||\varpi_{kpx}||_F^2}{2\kappa_{kpx}^2}, \frac{z_{\eta ky}||\varpi_{kpy}||_F^2}{2\kappa_{kpy}^2}\}$ with $\kappa_{kpx}>0$ and $\kappa_{kpy}>0$ being positive constants.

Combined with the virtual signals in (16)-(17) and the adaptive law in (18), we further have:

$$\dot{V}_{p1} \le -\sum_{k\in\mathscr{F}_{ag}} k_1 z_{\eta k}^{\top}e_{kp} - \sum_{k\in\mathscr{F}_a}\frac{k_{az}e_{kz}^2}{\eta_{kz}^2-e_{kz}^2} - \sum_{k\in\mathscr{F}_g}\frac{k_{g\psi}e_{k\psi}^2}{\eta_{k\psi}^2-e_{k\psi}^2}$$
$$+\sum_{k\in\mathscr{F}_g}\left(z_{\eta k}^{\top}((d_{nk}+b_{k0})(\bar{z}_{kv}+\frac{\partial\Xi_k}{\partial x_{k\psi}}\bar{\varphi}_k z_{k\omega})) + \frac{e_{k\psi}z_{k\omega}}{\eta_{k\psi}^2-e_{k\psi}^2}\right)$$
$$+\sum_{k\in\mathscr{F}_a}\left(z_{\eta k}^{\top}((d_{nk}+b_{k0})e_{k2}) + \frac{e_{kz}z_{kz}}{\eta_{kz}^2-e_{kz}^2}\right) + \sum_{k\in\mathscr{F}_{ag}}\frac{\varepsilon_{kp}}{\lambda_{kp}}\tilde{\vartheta}_{kp}^{\top}\hat{\vartheta}_{kp} + \upsilon_{p1}, \tag{23}$$

where $\bar{z}_{kv} = [z_{kv}\cos\psi_k, z_{kv}\sin\psi_k]^{\top}$, $\upsilon_{p1} = \sum_{k\in\mathscr{F}_{ag}}\frac{1}{2}(\kappa_{kpx}^2+\kappa_{kpy}^2+\bar{\delta}_{kpx}^2+\bar{\delta}_{kpy}^2)$.

Fault-tolerant control laws design. Let $z_{ka} = [e_{k2}^{\top}, z_{kz}]^{\top}$, from (10), the dynamics of z_{ka} is

$$\dot{z}_{ka} = -\zeta_{km}\dot{x}_{k1} + \frac{f_{ukp}}{m_k}\Theta_k + g_a + \frac{\sigma_{kp}}{m_k}u_{ka} - \dot{\alpha}_{ka}$$
$$= h_{kv} + \frac{\sigma_{kp}}{m_k}u_{ka}, \tag{24}$$

where $h_{kv} = -\zeta_{km}\dot{x}_{k1} + \frac{f_{ukp}}{m_k}\Theta_k + g_a - \dot{\alpha}_{ka}$. Similarly, the radial basis function neural network is adopted to approximate h_{kv}, we have $h_{kv} = \vartheta_{kv}^{*\top}\varpi_{kv}(\varsigma)+\sigma_{kv}(\varsigma)$, where $\vartheta_{kv}^{*\top} = \mathrm{diag}\{\vartheta_{kvx}^{*\top}, \vartheta_{kvy}^{*\top}, \vartheta_{kvz}^{*\top}\}$ and $\varpi_{kv} = [\varpi_{kvx}^{\top}, \varpi_{kvy}^{\top}, \varpi_{kvz}^{\top}]^{\top}$ denote the ideal weight vectors and the basis functions with $||\vartheta_{kvl}^{*\top}|| \le \bar{\vartheta}_{kvl}$ and $||\sigma_{kvx}(\varsigma)|| \le \bar{\sigma}_{kvl}, l = x,y,z$, respectively, $\sigma_{kv} = [\sigma_{kvx}, \sigma_{kvy}, \sigma_{kvz}]^{\top}$ is the approximation error.

Further, the adaptive fault-tolerant control signal $u_{ka}, k\in\mathscr{F}_a$ of the follower UAVs is designed as:

$$u_{ka} = \hat{\sigma}_{mk}\bar{u}_{ak},$$
$$\bar{u}_{ka} = -k_{a2}z_{ka} - \Xi_{k\varpi}^{v}\hat{\vartheta}_{kv} - \frac{1}{2}z_{\eta ka}^{v} - \Upsilon_{ka}, \tag{25}$$

where $\hat{\sigma}_{mk}$ is the estimate of σ_{mk}, $\sigma_{mk} = m_k/\sigma_{kp}$, $k_{a2}>0$ is the designed parameter, $z_{\eta ka}^{v} = [z_{\eta kx}^{v}, z_{\eta ky}^{v}, z_{\eta kz}^{v}]^{\top}$ with $z_{\eta kq}^{v} = \frac{z_{kaq}}{\eta_{kq}^{v2}-z_{kaq}^2}$, $|z_{kaq}| < \eta_{kq}^{v}, q = x,y,z$, $\eta_{kq}^{v}>0$ is the constraint value, $\Xi_{k\varpi}^{v} = \mathrm{diag}\{\frac{z_{\eta kq}^{v}||\varpi_{kvq}||_F^2}{2\kappa_{kvq}^2}\}$, $\kappa_{kvq}>0$ is the designed constant for $q = x,y,z$, $\hat{\vartheta}_{kv}$ is the estimate

of $\bar{\vartheta}_{kv} = [\bar{\vartheta}_{kvx}, \bar{\vartheta}_{kvy}, \bar{\vartheta}_{kvz}]^\top$, $\Upsilon_{ka} = [\Upsilon_{kx}, \Upsilon_{ky}, \Upsilon_{kz}]^\top$ with $\Upsilon_{kx} = -(d_{nk} + b_{k0}) z_{\eta kx} (\eta_{kx}^{v2} - z_{kax}^2)$, $\Upsilon_{ky} = -(d_{nk} + b_{k0}) z_{\eta ky} (\eta_{ky}^{v2} - z_{kay}^2)$, $\Upsilon_{kz} = -e_{kz}(\eta_{kz}^{v2} - z_{kz}^2)/(\eta_{kz}^2 - e_{kz}^2)$.

To construct the fault-tolerant control signal u_{ak}in (25), the adaptive update laws of $\hat{\sigma}_{mk}$ and $\hat{\bar{\vartheta}}_{kv}$, $k \in \mathscr{F}_a$ are chosen as:

$$\dot{\hat{\sigma}}_{mk} = -\lambda_{k\sigma} z_{\eta ka}^{v\top} \bar{u}_{ka} - \varepsilon_{k\sigma} \hat{\sigma}_{mk}, \tag{26}$$

$$\dot{\hat{\bar{\vartheta}}}_{kv} = \lambda_{kv} \Xi_{k\varpi}^{v} z_{\eta ka}^{v} - \varepsilon_{kv} \hat{\bar{\vartheta}}_{kv}, \tag{27}$$

where $\lambda_{k\sigma}$, λ_{kv}, $\varepsilon_{k\sigma}$ and ε_{kv} are positive constants.

Define the error variable $z_{kg} = [z_{kv}, z_{k\omega}]^\top$ for the kth follower UGV, from (10), the dynamics of z_{kg} is:

$$\begin{aligned} \dot{z}_{kg} &= -M_{Dk}\xi_k - M_{Ck}\omega_k\xi_k + M_{Rk} f_{\tau k} + M_{Rk}\sigma_k\tau_k - \dot{\alpha}_{kg} \\ &= h_{kv} + M_{Rk}\sigma_k\tau_k, \end{aligned} \tag{28}$$

where $h_{kv} = -M_{Dk}\xi_k - M_{Ck}\omega_k\xi_k + M_{Rk} f_{\tau k} - \dot{\alpha}_{kg}$. From $h_{kv} = \vartheta_{kv}^{*\top} \varpi_{kv}(\varsigma) + \sigma_{kv}(\varsigma)$, the adaptive fault-tolerant control signal $\tau_k, k \in \mathscr{F}_g$ of the follower UGVs is constructed as:

$$\begin{aligned} \tau_k &= \hat{\sigma}_k \bar{\tau}_k, \\ \bar{\tau}_k &= M_{Rk}^{-1}(-k_{g2} z_{kg} - \Xi_{k\varpi}^{v} \hat{\bar{\vartheta}}_{kv} - \frac{1}{2} z_{\eta kg}^{v} - \Upsilon_{kg}), \end{aligned} \tag{29}$$

where $\hat{\sigma}_k$ is the estimate of $\sigma_k = \mathrm{diag}\{\sigma_{k1}, \sigma_{k2}\}$, $k_{g2} > 0$ is the designed parameter, $z_{\eta kg}^{v} = [z_{\eta k1}^{v}, z_{\eta k2}^{v}]^\top$ with $z_{\eta k1}^{v} = \frac{z_{kg1}}{\eta_{k1}^{v2} - z_{kg1}^2}$ and $z_{\eta k2}^{v} = \frac{z_{kg2}}{\eta_{k2}^{v2} - z_{kg2}^2}$, $|z_{kg1}| < \eta_{k1}^{v}$, $|z_{kg2}| < \eta_{k2}^{v}$, $\eta_{k1}^{v} > 0$ and $\eta_{k2}^{v} > 0$ are constraint values, $\Xi_{k\varpi}^{v} = \mathrm{diag}\{\frac{z_{\eta k1}^{v} ||\varpi_{kv1}||_F^2}{2\kappa_{kv1}^2}, \frac{z_{\eta k2}^{v} ||\varpi_{kv2}||_F^2}{2\kappa_{kv2}^2}\}$, κ_{kv1} and κ_{kv2} are positive constants, $\hat{\bar{\vartheta}}_{kv}$ is the estimate of $\bar{\vartheta}_{kv} = [\bar{\vartheta}_{kv1}, \bar{\vartheta}_{kv2}]^\top$, $\Upsilon_{kg} = [\Upsilon_{kg1}, \Upsilon_{kg2}]^\top$, $\Upsilon_{kg1} = (d_{nk} + b_{k0}) z_{\eta k}^\top \Xi_{k\psi} (\eta_{k1}^{v2} - z_{kv}^2)$ and $\Upsilon_{kg2} = ((d_{nk} + b_{k0}) z_{\eta k}^\top \frac{\partial \Xi_k}{\partial x_{k\psi}} \bar{\varphi}_k + \frac{e_{k\psi}}{\eta_{k\psi} - e_{k\psi}^2})(\eta_{k2}^{v2} - z_{k\omega}^2)$.

To construct the fault-tolerant control signal $\tau_k$in (29), the adaptive update laws of $\hat{\sigma}_k$ and $\hat{\bar{\vartheta}}_{kv}$, $k \in \mathscr{F}_g$ are designed as:

$$\dot{\hat{\sigma}}_k = -\lambda_{k\sigma} \bar{\tau}_k M_{Rk}^\top z_{\eta kg}^{v\top} - \varepsilon_{k\sigma} \hat{\sigma}_k, \tag{30}$$

$$\dot{\hat{\bar{\vartheta}}}_{kv} = \lambda_{kv} \Xi_{k\varpi}^{v} z_{\eta kg}^{v} - \varepsilon_{kv} \hat{\bar{\vartheta}}_{kv}, \tag{31}$$

where $\lambda_{k\sigma}$, λ_{kv}, $\varepsilon_{k\sigma}$ and ε_{kv} are positive constants.

3.3. Fault-tolerant controller design for attitude subsystem of quadrotors

The adaptive FTC scheme with state constraints for position subsystems includes the kinematic control laws design and the dynamic control laws design.

Kinematic control laws design. From (11) and (12), the dynamics of the error variables is described below:

$$\dot{e}_{kr} = x_{k\omega} - \dot{x}_{0r}, k \in \mathscr{F}_a, \tag{32}$$

where $e_{kr} = [e_{k\phi}, e_{k\theta}, e_{k\psi}]^\top$, $x_{k\omega} = [\omega_{k\phi}, \omega_{k\theta}, \omega_{k\psi}]^\top = [\dot{\phi}_k, \dot{\theta}_k, \dot{\psi}_k]^\top$, $x_{0r} = [\phi_{kd}, \theta_{kd}, x_{0\psi}]^\top$ denoted the desired attitude information, and ϕ_{kd} and θ_{kd} can be obtained from the control input signal u_{ka} of the position subsystem.

Define the virtual error variables as $z_{kr} = \omega_{kr} - \alpha_{kr}$, $k \in \mathscr{F}_a$. Then, the virtual control law α_{kr} of the kth follower quadrotor UAV is designed as:

$$\alpha_{kr} = -k_{ar} e_{kr} + \dot{x}_{0r}, \tag{33}$$

where $k_{ar} > 0$ is a designed parameter.

Consider a positive candidate function V_{r1} to perform a preliminary analysis of α_{kr},

$$V_{r1} = \sum_{k\in\mathcal{F}_a} \frac{1}{2}(\log \frac{\eta_{k\phi}^2}{\eta_{k\phi}^2 - e_{k\phi}^2} + \log \frac{\eta_{k\theta}^2}{\eta_{k\theta}^2 - e_{k\theta}^2} + \log \frac{\eta_{k\psi}^2}{\eta_{k\psi}^2 - e_{k\psi}^2}), \tag{34}$$

where $|e_{k\phi}| < \eta_{k\phi}$, $|e_{k\theta}| < \eta_{k\theta}$ and $e_{k\psi} < \eta_{k\psi}$ with $\eta_{k\phi}$, $\eta_{k\theta}$ and $\eta_{k\psi}$ being the desired constraint values of attitude tracking error of follower UAVs.

From (33), the derivative of V_{r1} is:

$$\dot{V}_{r1} = -\sum_{k\in\mathcal{F}_a} k_{ar} z_{\eta kr}^\top e_{kr} + \sum_{k\in\mathcal{F}_a} z_{\eta kr}^\top z_{kr}, \tag{35}$$

where $z_{\eta kr} = [z_{\eta k\phi}, z_{\eta k\theta}, z_{\eta k\psi}]^\top$ with $z_{\eta k\phi} = \frac{e_{k\phi}}{\eta_{k\phi}^2 - e_{k\phi}^2}$, $z_{\eta k\theta} = \frac{e_{k\theta}}{\eta_{k\theta}^2 - e_{k\theta}^2}$, $z_{\eta k\psi} = \frac{e_{k\psi}}{\eta_{k\psi}^2 - e_{k\psi}^2}$.

Fault-tolerant control laws design. The adaptive fault-tolerant control law $u_{k\omega}, k \in \mathcal{F}_a$ of the follower UAVs is designed as:

$$\begin{aligned} u_{k\omega} &= \hat{\bar{\Gamma}}_{k\omega} \bar{u}_{k\omega}, \\ \bar{u}_{k\omega} &= G_{k\omega}^{-1}(-k_{a\omega} z_{kr} - W_{k\omega}^\top \hat{\bar{\varphi}}_{k\omega} - F_{k\omega a} + \dot{\alpha}_{kr} - \Upsilon_{kr}), \end{aligned} \tag{36}$$

where $\hat{\bar{\Gamma}}_{k\omega}$ is the estimate of $\bar{\Gamma}_{k\omega} = \mathrm{diag}\{\frac{1}{\sigma_{k\phi}}, \frac{1}{\sigma_{k\theta}}, \frac{1}{\sigma_{k\psi}}\}$, $k_{a\omega} > 0$ is a designed constant. $W_{k\omega}^\top = \begin{bmatrix} W_{k\zeta} & W_{kf} \end{bmatrix}$ with $W_{k\zeta} = \mathrm{diag}\{-\frac{\dot{\phi}_k}{I_{kx}}, -\frac{\dot{\theta}_k}{I_{ky}} - \frac{\dot{\psi}_k}{I_{kz}}\}$ and $W_{kf} = \mathrm{diag}\{\frac{1}{I_{kx}}, \frac{1}{I_{ky}}, \frac{1}{I_{kz}}\}$, $\hat{\bar{\varphi}}_{k\omega}$ is the estimate of $\bar{\varphi}_{k\omega} = [\zeta_{k\phi}, \zeta_{k\theta}, \zeta_{k\psi}, \bar{f}_{uk\phi}, \bar{f}_{uk\theta}, \bar{f}_{uk\psi}]^\top$, $F_{k\omega a} = [F_{k\omega a}^\phi, F_{k\omega a}^\theta, F_{k\omega a}^\psi]^\top$is the known term with $F_{k\omega a}^\phi = \frac{I_{ky} - I_{kz}}{I_{kx}} \dot{\theta}_k \dot{\psi}_k - \dot{\theta}_k \frac{J_{kr}}{I_{kx}} \Omega_{ka}$, $F_{k\omega a}^\theta = \frac{I_{kz} - I_{kx}}{I_{ky}} \dot{\psi}_k \dot{\phi}_k + \dot{\phi}_k \frac{J_{kr}}{I_{ky}} \Omega_{ka}$ and $F_{k\omega a}^\psi = \frac{I_{kx} - I_{ky}}{I_{kz}} \dot{\phi}_k \dot{\theta}_k$, $\Upsilon_{kr} = [\Upsilon_{k\phi}, \Upsilon_{k\theta}, \Upsilon_{k\psi}]^\top$ with $\Upsilon_{k\phi} = z_{\eta k\phi}(\eta_{k\phi}^{\omega 2} - z_{k\phi}^2)$, $\Upsilon_{k\theta} = z_{\eta k\theta}(\eta_{k\theta}^{\omega 2} - z_{k\theta}^2)$, $\Upsilon_{k\psi} = z_{\eta k\psi}(\eta_{k\psi}^{\omega 2} - z_{k\psi}^2)$.

To construct the fault-tolerant control signal $u_{k\omega}$ in (36), the adaptive update laws of $\hat{\bar{\Gamma}}_{k\omega}$ and $\hat{\bar{\varphi}}_{k\omega}$ are chosen as:

$$\dot{\hat{\bar{\Gamma}}}_{k\omega} = -\lambda_{k\Gamma} \bar{u}_{k\omega} z_{\eta k\omega}^\top - \varepsilon_{k\Gamma} \hat{\bar{\Gamma}}_{k\omega}, \tag{37}$$

$$\dot{\hat{\bar{\varphi}}}_{k\omega} = \lambda_{k\varphi} W_{k\omega} z_{\eta k\omega} - \varepsilon_{k\varphi} \hat{\bar{\varphi}}_{k\omega}, \tag{38}$$

where $z_{\eta k\omega} = [\frac{z_{k\phi}}{\eta_{k\phi}^{\omega 2} - z_{k\phi}^2}, \frac{z_{k\theta}}{\eta_{k\theta}^{\omega 2} - z_{k\theta}^2}, \frac{z_{k\psi}}{\eta_{k\psi}^{\omega 2} - z_{k\psi}^2}]^\top$, $|z_{kq}| < \eta_{kq}^\omega, q = \phi, \theta, \psi$, $\eta_{kq}^\omega > 0$, $\lambda_{k\Gamma}$, $\lambda_{k\varphi}$, $\varepsilon_{k\Gamma}$ and $\varepsilon_{k\varphi}$ are positive constants.

3.4. Performance analysis

The overall formation tracking control performance of the proposed fault-tolerant adaptive control signals with constraints is given as follows.

Theorem 1. For the UAVs-UGVs formation systems with actuator faults and state constraints, the adaptive control signals $u_{ka}(t)$ in (25), $u_{k\omega}(t)$ in (36) and $\tau_k(t)$ in (29) updated by the adaptive laws in (26)–(27), (37)–(38) and (30)–(31), it can be guaranteed that all closed-loop signals are uniformly ultimately bounded, and the errors e_{kp}, e_{kz}, $e_{k\psi}$ and e_{kr} can converge to a small adjustable neighborhood of the origin, and the full state variables of UAVs and UGVs can maintain the performance constraints.

Proof: Consider the Lyapunov function candidate as:

$$\begin{aligned} V = V_{p1} + V_{pz} &+ \sum_{k\in\mathcal{F}_a} \frac{\sigma_{kp}}{2\lambda_{k\sigma} m_k} \mathrm{tr}\{\tilde{\sigma}_{mk}^\top \tilde{\sigma}_{mk}\} + \sum_{k\in\mathcal{F}_g} \frac{1}{2\lambda_{k\sigma}} \mathrm{tr}\{\tilde{\sigma}_k^\top \tilde{\sigma}_k\} + \sum_{k\in\mathcal{F}_{ag}} \frac{1}{2\lambda_{kv}} \tilde{\vartheta}_{kv}^\top \tilde{\vartheta}_{kv} \\ &+ V_{r1} + V_{rz} + \sum_{k\in\mathcal{F}_a} \frac{1}{2\lambda_{k\Gamma}} \mathrm{tr}\{\tilde{\bar{\Gamma}}_{k\omega}^\top G_{k\omega} \tilde{\bar{\Gamma}}_{k\omega}\} + \sum_{k\in\mathcal{F}_a} \frac{1}{2\lambda_{k\varphi}} \tilde{\bar{\varphi}}_{k\omega}^\top \tilde{\bar{\varphi}}_{k\omega}, \end{aligned} \tag{39}$$

where $V_{pz}=\sum_{k\in\mathcal{F}_g}\frac{1}{2}(\log\frac{\eta_{k1}^{v2}}{\eta_{k1}^{v2}-z_{kg1}^2}+\log\frac{\eta_{k2}^{v2}}{\eta_{k2}^{v2}-z_{kg2}^2})+\sum_{k\in\mathcal{F}_a}\frac{1}{2}(\log\frac{\eta_{kx}^{v2}}{\eta_{kx}^{v2}-z_{kax}^2}+\log\frac{\eta_{ky}^{v2}}{\eta_{ky}^{v2}-z_{kay}^2}+\log\frac{\eta_{kz}^{v2}}{\eta_{kz}^{v2}-z_{kaz}^2})$,
$V_{rz}=\sum_{k\in\mathcal{F}_a}\frac{1}{2}(\log\frac{\eta_{k\phi}^{\omega 2}}{\eta_{k\phi}^{\omega 2}-z_{k\phi}^2}+\log\frac{\eta_{k\theta}^{\omega 2}}{\eta_{k\theta}^{\omega 2}-z_{k\theta}^2}+\log\frac{\eta_{k\psi}^{\omega 2}}{\eta_{k\psi}^{\omega 2}-z_{k\psi}^2})$.

Remark 2: In the performance analysis, the log-type quadratic barrier Lyapunov function in (39) is introduced to ensure that all states of follower UAVs and UGVs can satisfy the designed performance constraints. Although the non-quadratic Lyapunov function employed in [31] and [32] can increase the convergence speed of the system, we mainly focuses on solving the problems of heterogeneous system structures and cooperative formation of the UAVs-UGVs systems, as well as fault-tolerant control in the presence of actuator faults, and the log-type barrier Lyapunov function can also solve the state constraint problem. In addition, the quadratic Lyapunov functions are also a special case of non-quadratic Lyapunov functions, such as the log-type barrier Lyapunov function in [12], and the tan-type barrier Lyapunov function in [15], and they are used to solve the state constraint problems of nonlinear systems with adaptive control design, and the structure of the constraint-based fault-tolerant controller designed in this paper is also not complicated. Thus, a quadratic barrier Lyapunov function is applied to conduct the system performance analysis.

From (10) and (11), and together with (23) and (35), the time derivative of is:

$$\begin{aligned}\dot{V}=&\dot{V}_{p1}+\sum_{k\in\mathcal{F}_a}z_{\eta ka}^{v\top}(\vartheta_{kv}^{*\top}\varpi_{kv}+\delta_{kv}+\frac{\sigma_{kp}}{m_k}u_{ka})+\sum_{k\in\mathcal{F}_g}z_{\eta kg}^{v\top}(\vartheta_{kv}^{*\top}\varpi_{kv}+\delta_{kv}+M_{Rk}\sigma_k\tau_k)\\&-\sum_{k\in\mathcal{F}_a}\frac{\sigma_{kp}}{\lambda_{k\sigma}m_k}\mathrm{tr}\{\tilde{\sigma}_{mk}^{\top}\dot{\hat{\sigma}}_{mk}\}-\sum_{k\in\mathcal{F}_g}\frac{1}{\lambda_{k\sigma}}\mathrm{tr}\{\tilde{\sigma}_k^{\top}\dot{\hat{\sigma}}_k\}-\sum_{k\in\mathcal{F}_{ag}}\frac{1}{\lambda_{kv}}\tilde{\vartheta}_{kv}^{\top}\dot{\hat{\vartheta}}_{kv}+\dot{V}_{r1}\\&+\sum_{k\in\mathcal{F}_a}z_{\eta k\omega}^{\top}(F_{k\omega}+G_{k\omega}\Gamma_{k\omega}u_{k\omega}-\dot{\alpha}_{kr})-\sum_{k\in\mathcal{F}_a}\frac{1}{\lambda_{k\Gamma}}\mathrm{tr}\{\tilde{\bar{\Gamma}}_{k\omega}^{\top}G_{k\omega}\dot{\hat{\bar{\Gamma}}}_{k\omega}\}-\sum_{k\in\mathcal{F}_a}\frac{1}{\lambda_{k\varphi}}\tilde{\varphi}_{k\omega}^{\top}\dot{\hat{\varphi}}_{k\omega}.\end{aligned}\tag{40}$$

According to Young's inequality, one has:

$$\sum_{k\in\mathcal{F}_a}z_{\eta ka}^{v\top}\vartheta_{kv}^{*\top}\varpi_{kv}\le\sum_{k\in\mathcal{F}_a}z_{\eta ka}^{v\top}\Xi_{k\varpi}^{v}\bar{\vartheta}_{kv}+\sum_{k\in\mathcal{F}_a}\frac{1}{2}(\kappa_{kvx}^2+\kappa_{kvy}^2+\kappa_{kvz}^2),\tag{41}$$

$$\sum_{k\in\mathcal{F}_a}z_{\eta ka}^{v\top}\delta_{kv}\le\sum_{k\in\mathcal{F}_a}\frac{1}{2}z_{\eta ka}^{v\top}z_{\eta ka}^{v}+\sum_{k\in\mathcal{F}_a}\frac{1}{2}(\bar{\delta}_{kvx}^2+\bar{\delta}_{kvy}^2+\bar{\delta}_{kvz}^2),\tag{42}$$

$$\sum_{k\in\mathcal{F}_g}z_{\eta kg}^{v\top}\vartheta_{kv}^{*\top}\varpi_{kv}\le\sum_{k\in\mathcal{F}_g}z_{\eta kg}^{v\top}\Xi_{k\varpi}^{v}\bar{\vartheta}_{kv}+\sum_{k\in\mathcal{F}_a}\frac{1}{2}(\kappa_{kv1}^2+\kappa_{kv2}^2),\tag{43}$$

$$\sum_{k\in\mathcal{F}_g}z_{\eta kg}^{v\top}\delta_{kv}\le\sum_{k\in\mathcal{F}_g}\frac{1}{2}z_{\eta kg}^{v\top}z_{\eta kg}^{v}+\sum_{k\in\mathcal{F}_g}\frac{1}{2}(\bar{\delta}_{kv1}^2+\bar{\delta}_{kv2}^2).\tag{44}$$

Combined with the fault-tolerant control signals in (25), (29) and (36) and the adaptive

laws in (26)-(27), (30)-(31) and (37)-(38), we further have:

$$\begin{aligned}\dot{V} = &-\sum_{k\in\mathcal{F}_{ag}} k_1 z_{\eta k}^{\top} e_{kp} - \sum_{k\in\mathcal{F}_a} \frac{k_{az} e_{kz}^2}{\eta_{kz}^2 - e_{kz}^2} - \sum_{k\in\mathcal{F}_g} \frac{k_{g\psi} e_{k\psi}^2}{\eta_{k\psi}^2 - e_{k\psi}^2} + \sum_{k\in\mathcal{F}_{ag}} \frac{\varepsilon_{kp}}{\lambda_{kp}} \tilde{\vartheta}_{kp}^{\top} \hat{\vartheta}_{kp} + \upsilon_{p1} \\ &- \sum_{k\in\mathcal{F}_a} k_{a2} z_{\eta ka}^{v\top} z_{ka} - \sum_{k\in\mathcal{F}_g} k_{g2} z_{\eta kg}^{v\top} z_{kg} + \sum_{k\in\mathcal{F}_{ag}} \frac{\varepsilon_{kv}}{\lambda_{kv}} \tilde{\vartheta}_{kv}^{\top} \hat{\vartheta}_{kv} + \sum_{k\in\mathcal{F}_a} \frac{\varepsilon_{k\sigma}\sigma_{kp}}{\lambda_{k\sigma} m_k} \mathrm{tr}\{\tilde{\sigma}_{mk}^{\top} \hat{\sigma}_{mk}\} \\ &+ \sum_{k\in\mathcal{F}_g} \frac{\varepsilon_{k\sigma}}{\lambda_{k\sigma}} \mathrm{tr}\{\tilde{\sigma}_k^{\top} \hat{\sigma}_k\} + \upsilon_{p2} - \sum_{k\in\mathcal{F}_a} k_{ar} z_{\eta kr}^{\top} e_{kr} - \sum_{k\in\mathcal{F}_a} k_{a\omega} z_{\eta k\omega}^{\top} z_{kr} \\ &+ \sum_{k\in\mathcal{F}_a} \frac{\varepsilon_{k\Gamma}}{\lambda_{k\Gamma}} \mathrm{tr}\{\tilde{\bar{\Gamma}}_{k\omega}^{\top} G_{k\omega} \hat{\bar{\Gamma}}_{k\omega}\} + \sum_{k\in\mathcal{F}_a} \frac{\varepsilon_{k\varphi}}{\lambda_{k\varphi}} \tilde{\bar{\varphi}}_{k\omega}^{\top} \hat{\bar{\varphi}}_{k\omega}, \end{aligned} \tag{45}$$

where $\upsilon_{p2} = \sum_{k\in\mathcal{F}_a} \frac{1}{2}(\kappa_{kvx}^2 + \kappa_{kvy}^2 + \kappa_{kvz}^2) + \sum_{k\in\mathcal{F}_a} \frac{1}{2}(\bar{\delta}_{kvx}^2 + \bar{\delta}_{kvy}^2 + \bar{\delta}_{kvz}^2) + \sum_{k\in\mathcal{F}_g} \frac{1}{2}(\kappa_{kv1}^2 + \kappa_{kv2}^2) + \sum_{k\in\mathcal{F}_g} \frac{1}{2}(\bar{\delta}_{kv1}^2 + \bar{\delta}_{kv2}^2)$.

Using the Young's inequalities and the properties $\tilde{a}^{\top}\hat{a} \le -\frac{1}{2}\tilde{a}^{\top}\tilde{a} + \frac{1}{2}a^{\top}a$ with $\tilde{a} = a - \hat{a}$, one has:

$$\sum_{k\in\mathcal{F}_{ag}} \frac{\varepsilon_{kp}}{\lambda_{kp}} \tilde{\vartheta}_{kp}^{\top} \hat{\vartheta}_{kp} \le -\sum_{k\in\mathcal{F}_{ag}} \frac{\varepsilon_{kp}}{2\lambda_{kp}} \tilde{\vartheta}_{kp}^{\top} \tilde{\vartheta}_{kp} + \sum_{k\in\mathcal{F}_{ag}} \frac{\varepsilon_{kp}}{2\lambda_{kp}} \vartheta_{kp}^{\top} \vartheta_{kp}, \tag{46}$$

$$\sum_{k\in\mathcal{F}_a} \frac{\varepsilon_{k\sigma}\sigma_{kp}}{\lambda_{k\sigma} m_k} \tilde{\sigma}_{mk} \hat{\sigma}_{mk} \le -\sum_{k\in\mathcal{F}_a} \frac{\varepsilon_{k\sigma}\sigma_{kp}}{2\lambda_{k\sigma} m_k} \tilde{\sigma}_{mk}^2 + \sum_{k\in\mathcal{F}_a} \frac{\varepsilon_{k\sigma}\sigma_{kp}}{2\lambda_{k\sigma} m_k} \sigma_{mk}^2, \tag{47}$$

$$\sum_{k\in\mathcal{F}_g} \frac{\varepsilon_{k\sigma}}{\lambda_{k\sigma}} \mathrm{tr}\{\tilde{\sigma}_k^{\top} \hat{\sigma}_k\} \le -\sum_{k\in\mathcal{F}_g} \frac{\varepsilon_{k\sigma}}{2\lambda_{k\sigma}} \mathrm{tr}\{\tilde{\sigma}_k^{\top} \tilde{\sigma}_k\} + \sum_{k\in\mathcal{F}_g} \frac{\varepsilon_{k\sigma}}{2\lambda_{k\sigma}} \mathrm{tr}\{\sigma_k^{\top} \sigma_k\}, \tag{48}$$

$$\sum_{k\in\mathcal{F}_a} \frac{\varepsilon_{k\Gamma}}{\lambda_{k\Gamma}} \mathrm{tr}\{\tilde{\bar{\Gamma}}_{k\omega}^{\top} G_{k\omega} \hat{\bar{\Gamma}}_{k\omega}\} \le -\sum_{k\in\mathcal{F}_a} \frac{\varepsilon_{k\Gamma}}{2\lambda_{k\Gamma}} \mathrm{tr}\{\tilde{\bar{\Gamma}}_{k\omega}^{\top} G_{k\omega} \tilde{\bar{\Gamma}}_{k\omega}\} + \sum_{k\in\mathcal{F}_a} \frac{\varepsilon_{k\Gamma}}{2\lambda_{k\Gamma}} \mathrm{tr}\{\bar{\Gamma}_{k\omega}^{\top} G_{k\omega} \bar{\Gamma}_{k\omega}\}, \tag{49}$$

$$\sum_{k\in\mathcal{F}_a} \frac{\varepsilon_{k\varphi}}{\lambda_{k\varphi}} \tilde{\bar{\varphi}}_{k\omega}^{\top} \hat{\bar{\varphi}}_{k\omega} \le -\sum_{k\in\mathcal{F}_a} \frac{\varepsilon_{k\varphi}}{2\lambda_{k\varphi}} \tilde{\bar{\varphi}}_{k\omega}^{\top} \tilde{\bar{\varphi}}_{k\omega} + \sum_{k\in\mathcal{F}_a} \frac{\varepsilon_{k\varphi}}{2\lambda_{k\varphi}} \bar{\varphi}_{k\omega}^{\top} \bar{\varphi}_{k\omega}. \tag{50}$$

Then, we have:

$$\begin{aligned}\dot{V} = &-\sum_{k\in\mathcal{F}_{ag}} k_1 z_{\eta k}^{\top} e_{kp} - \sum_{k\in\mathcal{F}_a} \frac{k_{az} e_{kz}^2}{\eta_{kz}^2 - e_{kz}^2} - \sum_{k\in\mathcal{F}_g} \frac{k_{g\psi} e_{k\psi}^2}{\eta_{k\psi}^2 - e_{k\psi}^2} - \sum_{k\in\mathcal{F}_{ag}} \frac{\varepsilon_{kp}}{2\lambda_{kp}} \tilde{\vartheta}_{kp}^{\top} \tilde{\vartheta}_{kp} \\ &- \sum_{k\in\mathcal{F}_a} k_{a2} z_{\eta ka}^{v\top} z_{ka} - \sum_{k\in\mathcal{F}_g} k_{g2} z_{\eta kg}^{v\top} z_{kg} - \sum_{k\in\mathcal{F}_{ag}} \frac{\varepsilon_{kv}}{2\lambda_{kv}} \tilde{\vartheta}_{kv}^{\top} \tilde{\vartheta}_{kv} - \sum_{k\in\mathcal{F}_a} \frac{\varepsilon_{k\sigma}\sigma_{kp}}{2\lambda_{k\sigma} m_k} \tilde{\sigma}_{mk}^2 \\ &- \sum_{k\in\mathcal{F}_g} \frac{\varepsilon_{k\sigma}}{2\lambda_{k\sigma}} \mathrm{tr}\{\tilde{\sigma}_k^{\top} \tilde{\sigma}_k\} - \sum_{k\in\mathcal{F}_a} k_{ar} z_{\eta kr}^{\top} e_{kr} - \sum_{k\in\mathcal{F}_a} k_{a\omega} z_{\eta k\omega}^{\top} z_{kr} \\ &- \sum_{k\in\mathcal{F}_a} \frac{\varepsilon_{k\Gamma}}{2\lambda_{k\Gamma}} \mathrm{tr}\{\tilde{\bar{\Gamma}}_{k\omega}^{\top} G_{k\omega} \tilde{\bar{\Gamma}}_{k\omega}\} - \sum_{k\in\mathcal{F}_a} \frac{\varepsilon_{k\varphi}}{2\lambda_{k\varphi}} \tilde{\bar{\varphi}}_{k\omega}^{\top} \tilde{\bar{\varphi}}_{k\omega} + \upsilon, \end{aligned} \tag{51}$$

where $\upsilon = \sum_{k\in\mathcal{F}_{ag}} \frac{\varepsilon_{kp}}{2\lambda_{kp}} \vartheta_{kp}^{\top} \vartheta_{kp} + \sum_{k\in\mathcal{F}_{ag}} \frac{\varepsilon_{kv}}{2\lambda_{kv}} \vartheta_{kv}^{\top} \vartheta_{kv} + \sum_{k\in\mathcal{F}_a} \frac{\varepsilon_{k\sigma}\sigma_{kp}}{2\lambda_{k\sigma} m_k} \sigma_{mk}^2 + \sum_{k\in\mathcal{F}_g} \frac{\varepsilon_{k\sigma}}{2\lambda_{k\sigma}} \mathrm{tr}\{\sigma_k^{\top} \sigma_k\} + \sum_{k\in\mathcal{F}_a} \frac{\varepsilon_{k\Gamma}}{2\lambda_{k\Gamma}} \mathrm{tr}\{\bar{\Gamma}_{k\omega}^{\top} G_{k\omega} \bar{\Gamma}_{k\omega}\} + \sum_{k\in\mathcal{F}_a} \frac{\varepsilon_{k\varphi}}{2\lambda_{k\varphi}} \bar{\varphi}_{k\omega}^{\top} \bar{\varphi}_{k\omega} + \upsilon_{p1} + \upsilon_{p2}$.

According to [33], one has $\log\frac{\eta_{kz}^2}{\eta_{kz}^2-e_{kz}^2}\leq\frac{e_{kz}^2}{\eta_{kz}^2-e_{kz}^2}$, it yields,

$$\begin{aligned}\dot{V}=&-k_1\sum_{k\in\mathscr{F}_{ag}}(\log\frac{\eta_{kx}^2}{\eta_{kx}^2-e_{kpx}^2}+\log\frac{\eta_{ky}^2}{\eta_{ky}^2-e_{kpy}^2})-\sum_{k\in\mathscr{F}_{ag}}\left(\frac{\varepsilon_{kp}}{2\lambda_{kp}}\tilde{\vartheta}_{kp}^{\top}\tilde{\vartheta}_{kp}+\frac{\varepsilon_{kv}}{2\lambda_{kv}}\tilde{\vartheta}_{kv}^{\top}\tilde{\vartheta}_{kv}\right)\\&-k_{az}\sum_{k\in\mathscr{F}_a}\log\frac{\eta_{kz}^2}{\eta_{kz}^2-e_{kz}^2}-k_{g\psi}\sum_{k\in\mathscr{F}_g}\log\frac{\eta_{k\psi}^2}{\eta_{k\psi}^2-e_{k\psi}^2}-k_{a2}\sum_{k\in\mathscr{F}_a}V_{va}-k_{g2}\sum_{k\in\mathscr{F}_g}V_{vg}\\&-\sum_{k\in\mathscr{F}_a}\frac{\varepsilon_{k\sigma}\sigma_{kp}}{2\lambda_{k\sigma}m_k}\tilde{\sigma}_{mk}^2-\sum_{k\in\mathscr{F}_g}\frac{\varepsilon_{k\sigma}}{2\lambda_{k\sigma}}\mathrm{tr}\{\tilde{\sigma}_k^{\top}\tilde{\sigma}_k\}-k_{a\omega}\sum_{k\in\mathscr{F}_a}V_{\omega a}-\sum_{k\in\mathscr{F}_a}\frac{\varepsilon_{k\Gamma}}{2\lambda_{k\Gamma}}\mathrm{tr}\{\tilde{\bar{\Gamma}}_{k\omega}^{\top}G_{k\omega}\tilde{\bar{\Gamma}}_{k\omega}\}\\&-k_{ar}\sum_{k\in\mathscr{F}_{ag}}(\log\frac{\eta_{k\phi}^2}{\eta_{k\phi}^2-e_{k\phi}^2}+\log\frac{\eta_{k\theta}^2}{\eta_{k\theta}^2-e_{k\theta}^2}+\log\frac{\eta_{k\psi}^2}{\eta_{k\psi}^2-e_{k\psi}^2})-\sum_{k\in\mathscr{F}_a}\frac{\varepsilon_{k\varphi}}{2\lambda_{k\varphi}}\tilde{\bar{\varphi}}_{k\omega}^{\top}\tilde{\bar{\varphi}}_{k\omega}+\upsilon,\end{aligned}\tag{52}$$

where $V_{va}=\log\frac{\eta_{kx}^{v2}}{\eta_{kx}^{v2}-z_{kax}^2}+\log\frac{\eta_{ky}^{v2}}{\eta_{ky}^{v2}-z_{kay}^2}+\log\frac{\eta_{kz}^{v2}}{\eta_{kz}^{v2}-z_{kaz}^2}$, $V_{vg}=\log\frac{\eta_{k1}^{v2}}{\eta_{k1}^{v2}-z_{kg1}^2}+\log\frac{\eta_{k2}^{v2}}{\eta_{k2}^{v2}-z_{kg2}^2}$, $V_{\omega a}=\log\frac{\eta_{k\phi}^{\omega 2}}{\eta_{k\phi}^{\omega 2}-z_{k\phi}^2}+\log\frac{\eta_{k\theta}^{\omega 2}}{\eta_{k\theta}^{\omega 2}-z_{k\theta}^2}+\log\frac{\eta_{k\psi}^{\omega 2}}{\eta_{k\psi}^{\omega 2}-z_{k\psi}^2}$.

Finally, it can be obtained that

$$\dot{V}\leq-\beta V+\upsilon,\tag{53}$$

where $\beta=2\min\{k_1,k_{az},k_{g\psi},k_{a2},k_{g2},k_{ar},k_{a\omega},\Pi_{\varepsilon 1},\Pi_{\varepsilon 2}\}$, $\Pi_{\varepsilon 1}=\{\varepsilon_{kp},\varepsilon_{kv},\varepsilon_{k\sigma}\},k\in\mathscr{F}_{ag}$, $\Pi_{\varepsilon 2}=\{\varepsilon_{k\Gamma},\varepsilon_{k\varphi}\},k\in\mathscr{F}_a$.

From (53), one can obtain that the tracking error signals $e_{kp},k\in\mathscr{F}_{ag}$, $e_{kz},e_{kr},k\in\mathscr{F}_a$, $e_{k\psi},k\in\mathscr{F}_g$ and the estimation errors $\tilde{\bar{\vartheta}}_{kp},\tilde{\bar{\vartheta}}_{kv},k\in\mathscr{F}_{ag}$, $\tilde{\sigma}_{mk},\tilde{\bar{\Gamma}}_{k\omega},\tilde{\bar{\varphi}}_{k\omega},k\in\mathscr{F}_a$, $\tilde{\sigma}_k,k\in\mathscr{F}_g$ are bounded. It can be further obtained that the control signals $\alpha_{ka},u_{ka},\alpha_{kr},u_{k\omega},k\in\mathscr{F}_a$ and $\alpha_{kg},\tau_k,k\in\mathscr{F}_g$ are bounded.

Since the neighborhood synchronization error e_{kp} is bounded, the formation tracking error $x_p-\gamma-\bar{x}_0$ satisfies $||x_p-\gamma-\bar{x}_0||\leq\frac{||e_p||}{\sigma_{\max}((L+B)\otimes I_2)}$, where $x_p=[x_{1p}^{\top},\ldots,x_{N+Mp}^{\top}]^{\top}$, $\gamma=[\gamma_1^{\top},\ldots,\gamma_{N+M}^{\top}]^{\top}$, $\bar{x}_0=[x_0^{\top},\ldots,x_0^{\top}]^{\top}\in R^{N+M}$, $e_p=[e_{1p}^{\top},\ldots,e_{N+Mp}^{\top}]^{\top}$. As $||x_p-\gamma-\bar{x}_0||\leq\frac{e_p}{\sigma_{\max}((L+B)\otimes I_2)}$, we have $|p_{kx}|-|\gamma_{kx}|-|f_{0x}|\leq\frac{||e_p||}{\sigma_{\max}((L+B)\otimes I_2)}$ and $|p_{ky}|-|\gamma_{ky}|-|f_{0y}|\leq\frac{||e_p||}{\sigma_{\max}((L+B)\otimes I_2)}$. Then, by choosing $\bar{\chi}_{kx}\geq\frac{||e_p||}{\sigma_{\max}((L+B)\otimes I_2)}+M_{\gamma kx}+M_{0x}$ and $\bar{\chi}_{ky}\geq\frac{||e_p||}{\sigma_{\max}((L+B)\otimes I_2)}+M_{\gamma ky}+M_{0y}$, it yields, $|p_{kx}|\leq\bar{\chi}_{kx}$ and $|p_{ky}|\leq\bar{\chi}_{ky}$, i.e., the state constraints can be guaranteed. Similarly, through selecting the appropriate parameters, the constrains of p_{kz}, x_{kr} for each follower UAV and $x_{k\psi}$ for each follower UGV can be obtained. From the previous analysis, the virtual control signals α_{ka}, α_{kg} and α_{kr} are bounded. It is supposed that $|\alpha_{kal}|\leq\bar{\alpha}_{kal},l=x,y,z,k\in\mathscr{F}_a$, $|\alpha_{kq}|\leq\bar{\alpha}_{kq},q=v,\omega,k\in\mathscr{F}_g$ and $|\alpha_{ks}|\leq\bar{\alpha}_{ks},s=\phi,\theta,\psi,k\in\mathscr{F}_a$ with $\bar{\alpha}_{kal}>0$, $\bar{\alpha}_{kq}>0$ and $\bar{\alpha}_{ks}>0$, respectively. Since $|z_{kal}|<\eta_{kl}^v,l=x,y,z$, $|z_{kv}|\leq\eta_{k1}^v,|z_{k\omega}|\leq\eta_{k2}^v$, $|z_{ks}|\leq\eta_{ks}^{\omega},s=\phi,\theta,\psi$, one has $|\dot{p}_{kl}|\leq\bar{\chi}_{kl}^v,l=x,y,z,|\omega_{ks}|\leq\bar{\chi}_{ks}^v,s=\phi,\theta,\psi$ for the kth follower UAV and $|v_k|\leq\bar{\chi}_{kv},|\omega_k|\leq\bar{\chi}_{k\omega}$ for the kth follower UGV. Therefore, all state variables of quadrotor UAVs and mobile robot UGVs satisfy the performance constraints. The proof is completed.

4. Simulation study

To show the effective fault-tolerant and state constraints performance of the proposed cooperative adaptive FTC control scheme, a numerical simulation for the UAVs-UGVs collaborative formation system are presented in this section,

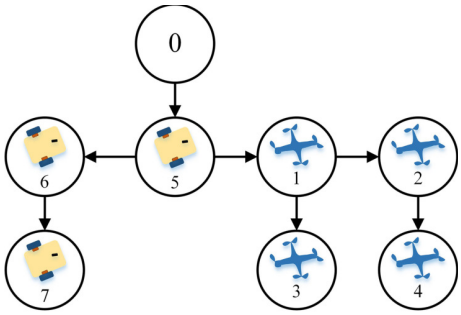

Figure 1. Communication topology.

4.1. Simulation conditions

The information communication among the UAVs-UGVs collaborative formation system is expressed by the digraph Ξ in Figure 1, where agents 1-4 denote four follower UAVs, agents 5-7 denote three follower UGVs, and agent 0 represents the virtual leader. The weight of each communication link between two agents equals to one.

Then, the system physical parameters of the quadrotor UAVs and mobile robot UGVs are given below: (1) the system parameters of follower quadrotor UAVs are considered as $m_k = 2\text{kg}, \zeta_{kx} = \zeta_{ky} = \zeta_{kz} = 0.012\text{N}\cdot\text{s/rad}$, $I_{kx} = I_{ky} = 1.25\text{N}\cdot\text{s}^2/\text{rad}$, $I_{kz} = 2.5\text{N}\cdot\text{s}^2/\text{rad}$, $I_{kr} = 0.001\text{kg}\cdot\text{m}^2$, $\zeta_\phi = \zeta_\theta = \zeta_\psi = 0.012\text{N}\cdot\text{s/rad}, k = 1,2,3,4$. (2) the system parameters of three mobile robot UGVs are considered as $h_k = 0.75\text{m}, r_k = 0.25\text{m}, m_{kc} = 10\text{kg}, m_{k\omega} = 1\text{kg}, I_{kc} = 5.6, I_{k\omega} = 0.005, I_{km} = 0.0025, c_{kg} = 0.3\text{m}, D_{k1} = D_{k2} = 5, k = 5,6,7$. The dynamic trajectory x_0 is considered as $x_0 = [t, 3\sin(0.5t)]^\top$, and the expected heading angle $x_{0\psi}$ is described as $x_{0\psi} = \arctan(\dot{x}_{0y}/\dot{x}_{0x})$. The desired cooperative height x_{0z} of each follower UAV is given by $x_{0z} = 6$. The expected geometrical formation structure is selected as $\gamma_k = [4\cos((k-1)\pi/2), 4\sin((k-1)\pi/2)]^\top, k = 1,\ldots,4$ and $\gamma_k = [2\cos((k-5)\pi/1.5), 2\sin((k-5)\pi/1.5)]^\top, k = 5,6,7$. In this simulation of the UAVs-UGVs formation systems, all follower vehicles are required to track the trajectory formed by the virtual leader 0 and achieve the desired geometric configuration and maintain the state performance constraints subject to actuator faults under the proposed adaptive FTC strategy.

The actuator faults are simulated as:

$$\begin{aligned}
&u_{2pf}(t) = 0.5u_{2p}(t) + 2\sin(t), \text{for } t \geq 15\text{s};\\
&u_{3\phi f}(t) = 0.6u_{3\phi}(t), u_{3\psi f}(t) = 0.55u_{3\psi}(t), \text{for } t \geq 25\text{s};\\
&\tau_{51f}(t) = 0.45\tau_{51}(t) + 1.5\sin(t), \tau_{52f}(t) = 0.5\tau_{52}(t), \text{for } t \geq 15\text{s};
\end{aligned} \tag{54}$$

which indicate that 1) the control thrust of UAV 2 loses its effectiveness from 100% to 50% and has a bias fault at $t = 15$s, the roll and yaw subsystem of UAV 3 loses its effectiveness from 100% to 60% and 100% to 55% at $t = 25$s; 2) in UGV 5, the control torque of left wheel loses its effectiveness from 100% to 45% and has a time-varying bias fault and the control torque of right wheel loses its effectiveness from 100% to 50% from $t = 15$s.

The initial conditions are chosen as $x_{11}(0) = [1.5, 0.8, 5.5]^\top$, $x_{21}(0) = [0.8, 2.5, 5.8]^\top$, $x_{31}(0) = [0.6, 2, 6.5]^\top, x_{41}(0) = [1.2, 1.2, 3.5]^\top, x_{51}(0) = [2.5, 1.5, 0.2]^\top, x_{61}(0) = [1.5, 0.8, 0.5]^\top$, $x_{71}(0) = [0.7, 1.6, 0.2]^\top$, $x_{1r}(0) = [0.2, 0.3, 0.4]^\top$, $x_{2r}(0) = [0.1, 0.25, 0.7]^\top$, $x_{3r}(0) = [-0.1, 0.6, 0.3]^\top$, $x_{4r}(0) = [-0.3, 0.7, 1]^\top$. $\hat{\vartheta}_{kp}(0) = [0.1, 0.1]^\top, \hat{\sigma}_{mk}(0) = 0, \hat{\vartheta}_{kv}(0) = [0.1, 0.1, 0.1]^\top, \hat{\bar{\Gamma}}_{k\omega}(0) = \text{diag}\{0,0,0\}, \hat{\varphi}_{k\omega}(0) = [0.1, 0.1, 0.1, 0.1, 0.1, 0.1]^\top$ for $k \in \mathscr{F}_a$, $\hat{\sigma}_k(0) = \text{diag}\{0,0\}, \hat{\bar{\vartheta}}_{kv}(0) = [0.1, 0.1]^\top$ for $k \in \mathscr{F}_g$. The gains in the control signals and adaptive laws are chosen as $k_1 = 2, k_{az} = 2, k_{g\psi} = 2, k_{ar} = 3, \lambda_{kp} = \lambda_{kv} = \lambda_{k\sigma} = 1, \varepsilon_{kp} = \varepsilon_{kv} = \varepsilon_{k\sigma} = 0.1$, for $k \in \mathscr{F}_{ag}$, $\lambda_{k\Gamma} = \lambda_{k\varphi} = 1.5, \varepsilon_{k\Gamma} = \varepsilon_{k\varphi} = 0.1$ for $k \in \mathscr{F}_a$.

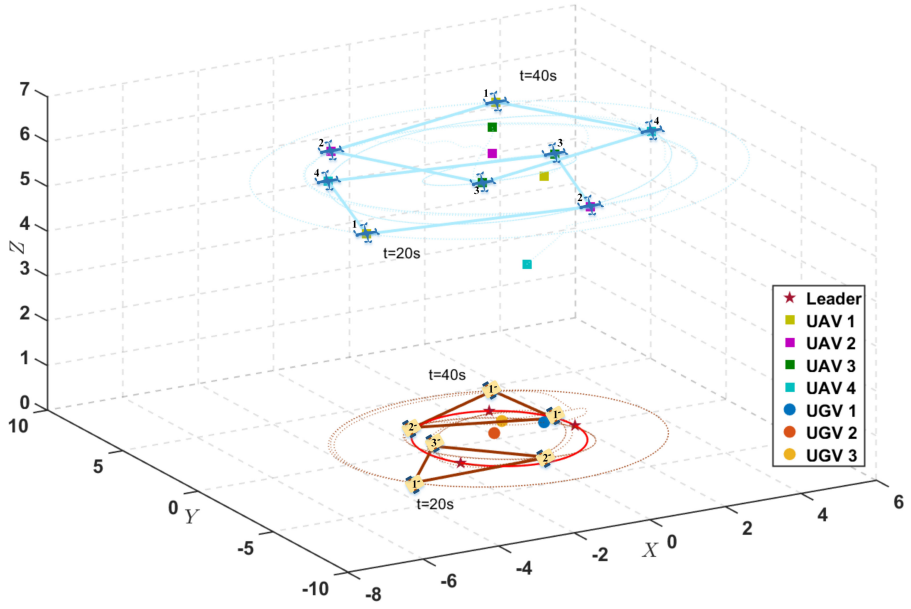

Figure 2. Tracking trajectories of follower vehicles in XYZ plane.

4.2. Simulation results

The following simulation results are presented to show the control performance of the proposed adaptive FTC algorithm with state constraints. Figure 2 and Figure 3 show the position tracking trajectories with geometric formation structure of the UAVs-UGVs formation systems in XYZ plane and XY plane, respectively, where the red "$\star$" represents the position of the virtual leader, the "■" and "●" in different colors represent the initial positions of follower UAVs and follower UGVs, respectively, the solid red line represents the movement trajectory of the virtual leader, and the dashed line represents the movement trajectory of followers. It can be seen from figures that during the formation movement of UAVs and UAVs, the follower UAVs and UAVs achieve the desired geometric formation configurations, such as the quadrilateral and triangular formation configurations formed at $t = 20$s and $t = 40$s, respectively. Thus, we can obtain that all follower UAVs and UAVs can perform an effective formation tracking with the developed cooperative adaptive FTC scheme under the influence of actuator faults. Figure 4 shows the neighborhood formation tracking errors of the position and attitude subsystems of follower UAVs, when the position subsystems of UAV 2 and the attitude subsystems of UAV 3 suffer from actuator faults at $t = 15$s and $t = 25$s, respectively, the neighborhood formation tracking errors $e_{2px}, e_{2py}, e_{2pz}$ and the attitude tracking errors $e_{3\phi}, e_{3\psi}$ can converge to a small adjustable neighborhood of the origin after the transient deviation. Figure 5 shows the neighborhood formation tracking errors of the follower UGVs, which indicates that the cooperative formation tracking performance of UGV 1 recovers after a transient response when the actuator faults occur at $t = 15$s. For comparison purposes, the formation tracking error performance indexes of follower UAV 2 and UAV 3 and follower UGV 1 in the presence of existing control scheme are also plotted in Figure 6 and Figure 7. It is clear that the proposed cooperative adaptive FTC method provides better convergency for the synchronization errors under the influence of same actuator faults. Figure 8 show the position variables and attitude variables of follower UAVs, it can be obtained that the system states p_{kx}, p_{ky}, p_{kz}, ϕ_k, θ_k and $\psi_k, k = 1,2,3,4$ can satisfy the predesigned performance constrains even when the actuator faults occur, and from Figure 9, the position and orientation variables p_{kx}, p_{ky} and $x_{k\phi}, k = 1,2,3$ can also maintain within the designed performance requirements.

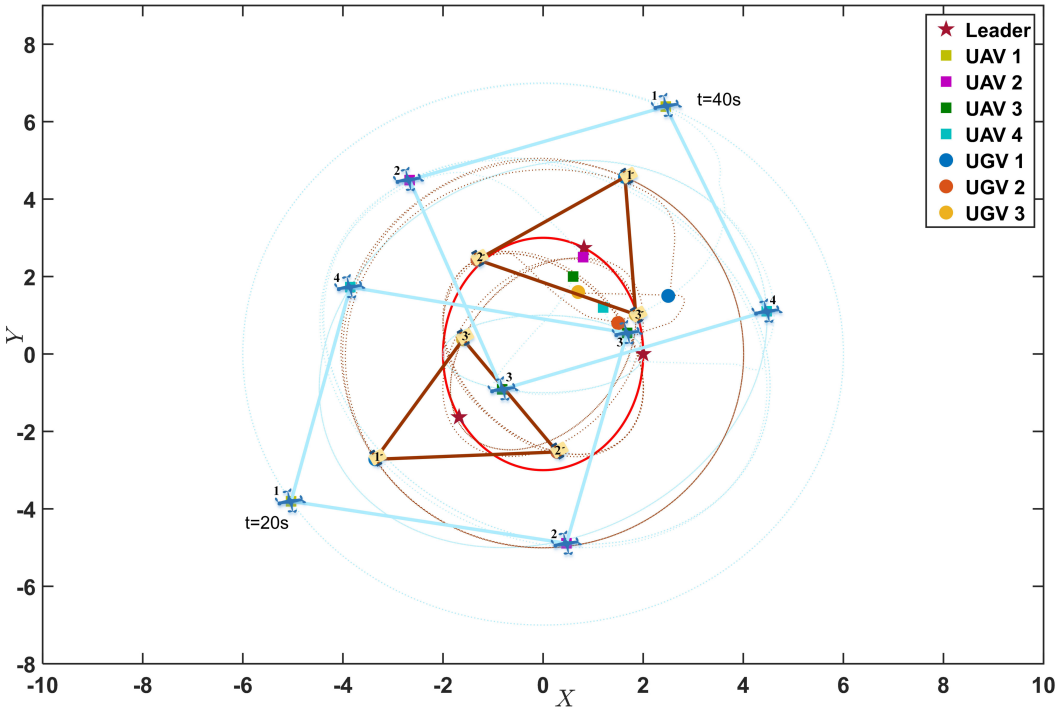

Figure 3. Tracking trajectories of follower vehicles in XY plane.

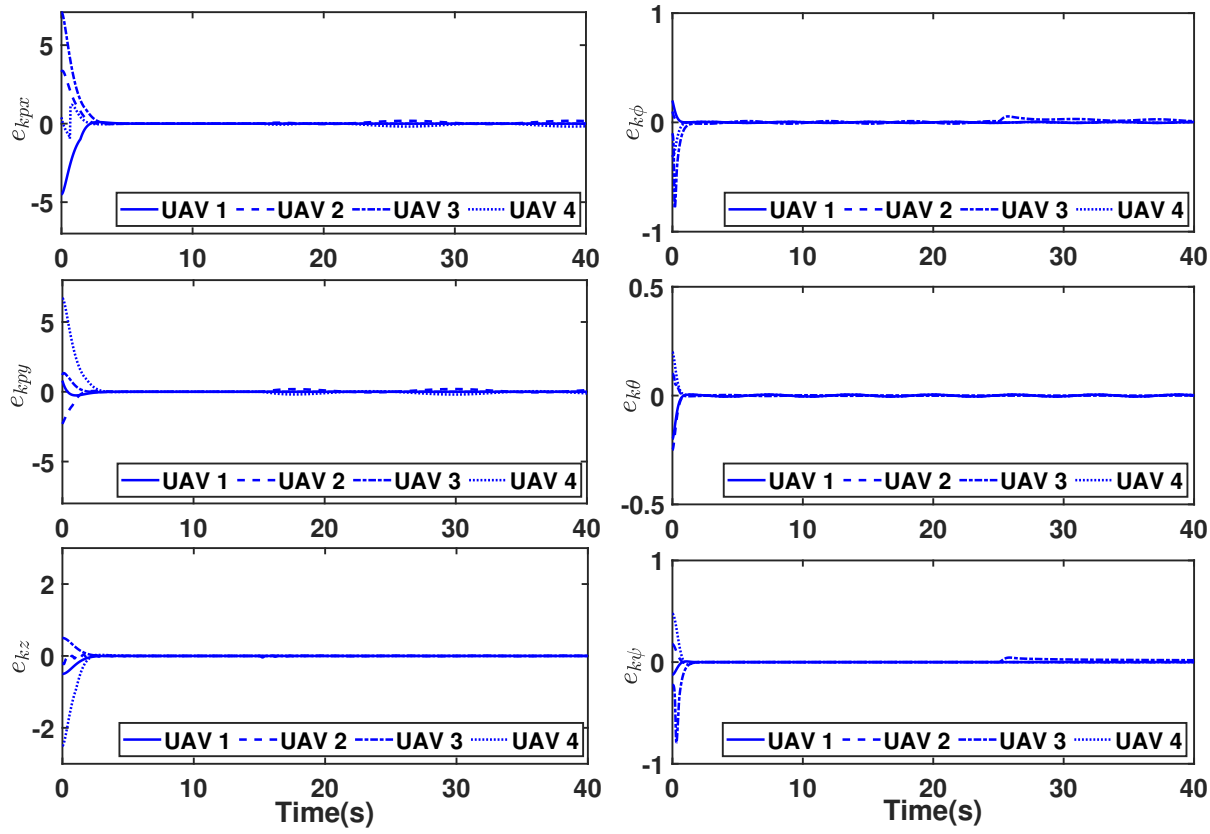

Figure 4. Formation tracking errors of five follower UAVs.

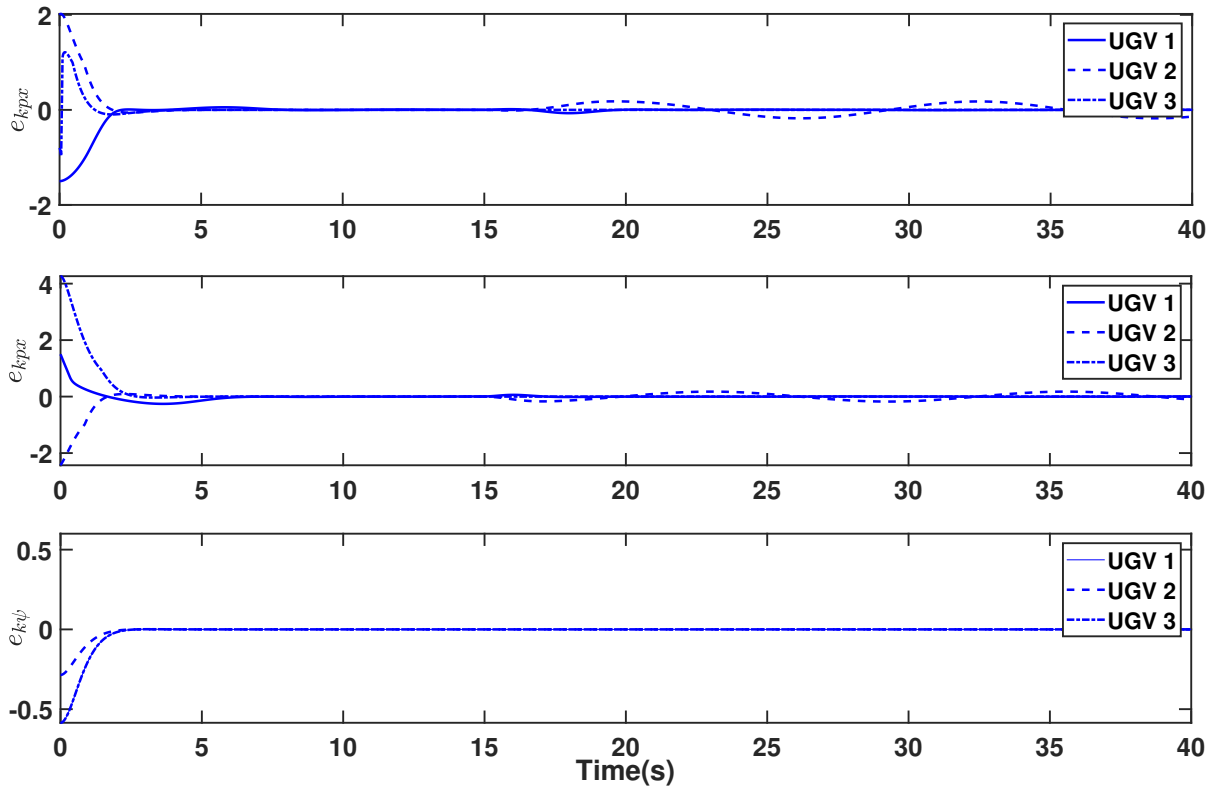

Figure 5. Formation tracking errors of three follower UGVs.

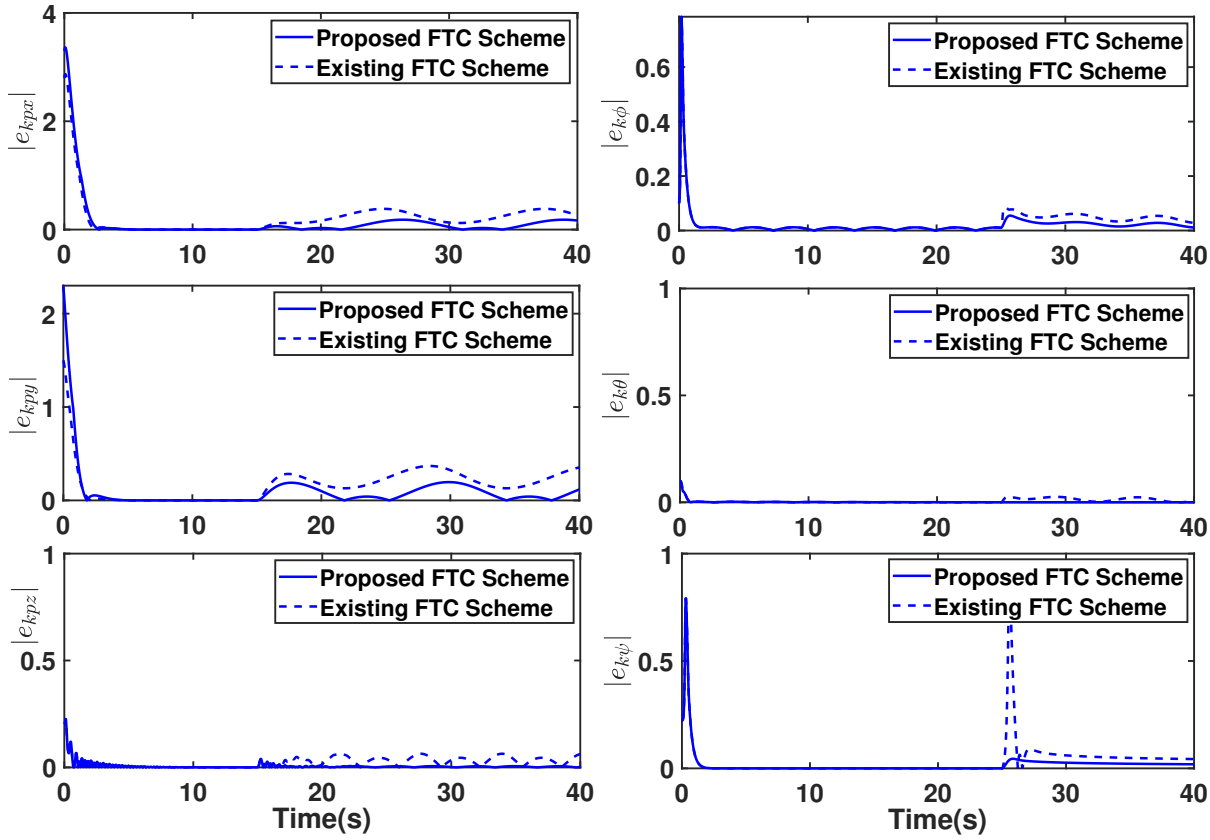

Figure 6. Formation tracking error performance indexes of faulty UAVs.

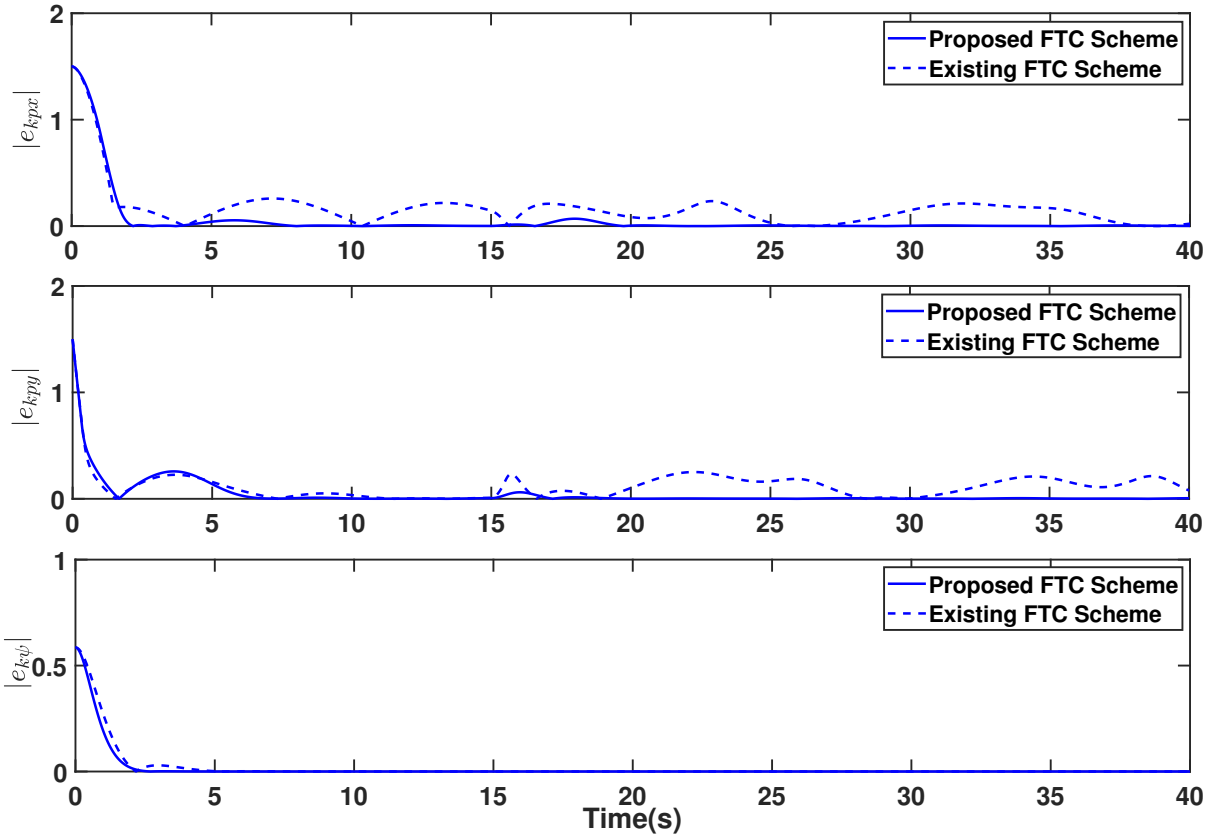

Figure 7. Formation tracking error performance indexes of faulty UGVs.

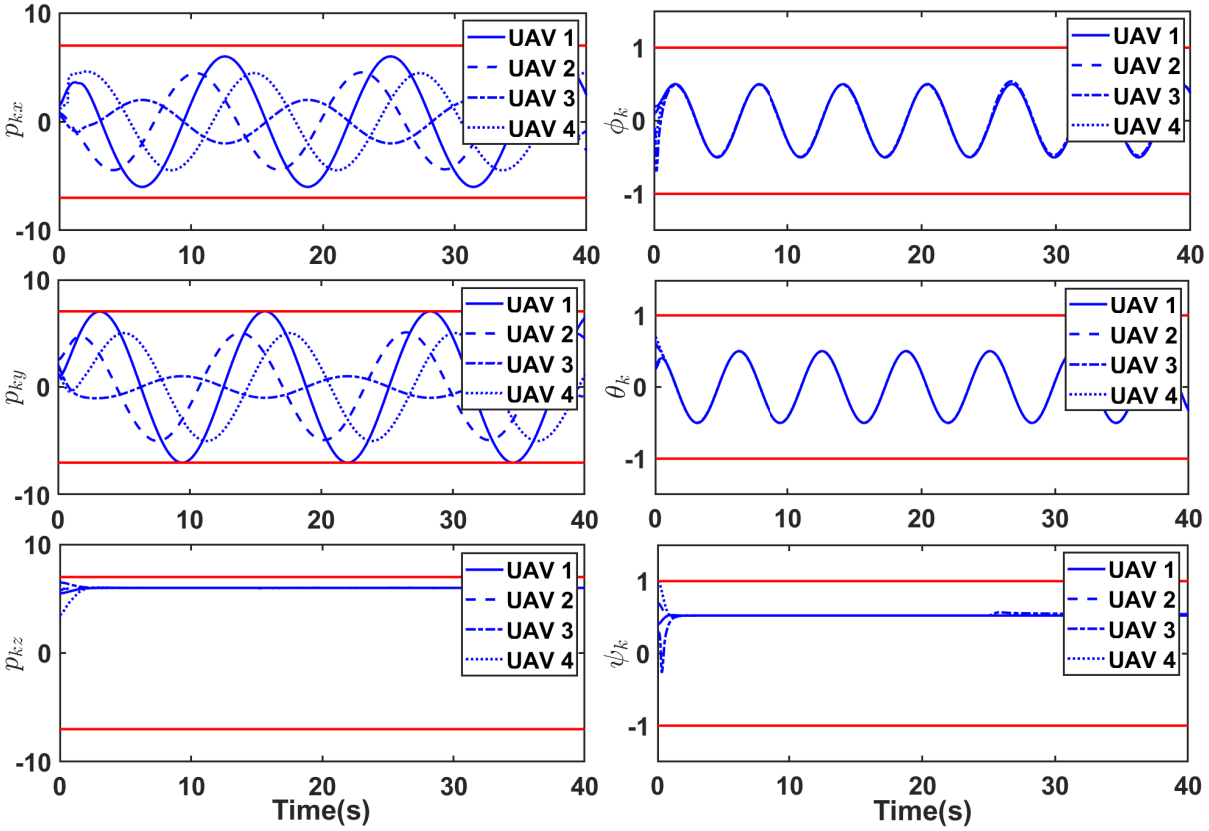

Figure 8. The position and attitude variables of follower UAVs.

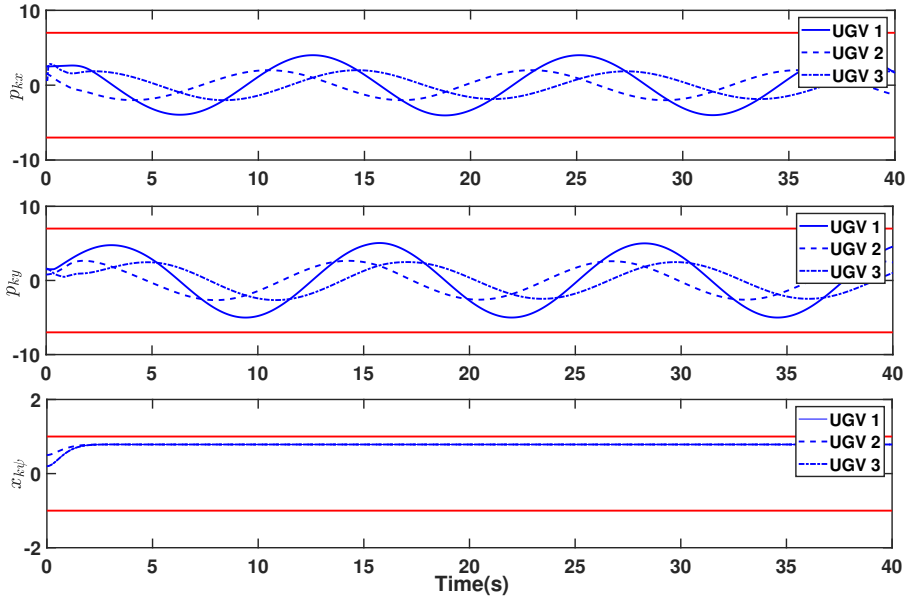

Figure 9. The position and orientation variables of follower UGVs.

5. Conclusion

In this paper, a cooperative adaptive FTC scheme is presented for the UAVs-UGVs formation systems with full-state constrains and actuator faults. By using the proposed method, the system achieves a good fault tolerance performance while the system states of quadrotor UAVs and mobile robot UGVs do not exceed the boundaries of the performance constraints. The simulation study shows the constraints and fault-tolerance performance of the presented adaptive FTC scheme. However, the types of faults considered in this paper are relatively simple and do not take into account the uncertain time-varying characteristics of the control gain matrix caused by time-varying faults, as well as the effects of network communication faults among agents. In the future work, we will investigate the constrains-based cooperative FTC control problem for the UAVs-UGVs formation systems with multiple complex faults.

Acknowledgments

This work was supported by the National Natural Science Foundation of China under Grant 62303293, 62303414, and the China Postdoctoral Science Foundation under Grant 2023M732176, 2023M741821, and the Natural Science Foundation of Zhejiang Province under Grant LQ23F030016.

Conflicts of interests

No potential conflict of interest was reported by the authors.

Author's contribution

Conceptualization, Jianye Gong, and Xiuli Wang; Writing—original draft preparation, Jianye Gong, and Xiuli Wang; Reviewing and editing, Yang Li, and Dandan Lyu; Methodology, Jianye Gong, and Xiuli Wang; Writing, Dandan Lyu. All authors have read and agreed to the published version of the manuscript.

References

[1] Yang T, Jiang Z, Sun R, Cheng N, Feng H. Maritime search and rescue based on group mobile computing for unmanned aerial vehicles and unmanned surface vehicles. *IEEE Trans. Ind. Inform.* 2020, 16(12):7700–7708.

[2] Maini P, Sundar K, Singh M, Rathinam S, Sujit P. Cooperative aerial–ground vehicle route planning with fuel constraints for coverage applications. *IEEE Trans. Aerosp. Electron. Syst.* 2019, 55(6):3016–3028.

[3] Shi P, Yan B. A survey on intelligent control for multiagent systems. *IEEE Trans. Syst. Man Cybern. Syst.* 2020, 51(1):161–175.

[4] Liu H, Tian Y, Lewis FL. Robust trajectory tracking in satellite time-varying formation flying. *IEEE Trans. Cybern.* 2020, 51(12):5752–5760.

[5] Lu M, Liu L. Leader-following attitude consensus of multiple rigid spacecraft systems under switching networks. *IEEE Trans. Autom. Control* 2019, 65(2):839–845.

[6] Turan E, Speretta S, Gill E. Autonomous navigation for deep space small satellites: Scientific and technological advances. *Acta Astronaut.* 2022, 193:56–74.

[7] Hua Y, Dong X, Hu G, Li Q, Ren Z. Distributed time-varying output formation tracking for heterogeneous linear multiagent systems with a nonautonomous leader of unknown input. *IEEE Trans. Autom. Control* 2019, 64(10):4292–4299.

[8] Zhao W, Liu H, Valavanis KP, Lewis FL. Fault-tolerant formation control for heterogeneous vehicles via reinforcement learning. *IEEE Trans. Aerosp. Electron. Syst.* 2021, 58(4):2796–2806.

[9] Gong J, Ma Y, Jiang B, Mao Z. Distributed adaptive fault-tolerant formation control for heterogeneous multiagent systems under switching directed topologies. *J. Frankl. Inst.* 2022, 359(8):3366–3388.

[10] Qu F, Tong S, Li Y. Observer-based adaptive fuzzy output constrained control for uncertain nonlinear multi-agent systems. *Inf. Sci.* 2018, 467:446–463.

[11] Yuan F, Liu YJ, Liu L, Lan J, Li D, *et al.* Adaptive neural consensus tracking control for nonlinear multiagent systems using integral barrier Lyapunov functionals. *IEEE Trans. Neural Netw. Learn. Syst.* 2021, 34(8):4544–4554.

[12] Yan L, Liu Z, Chen CP, Zhang Y, Wu Z. Distributed adaptive fuzzy containment control for state-constrained multiagent systems with uncertain leaders. *IEEE Trans. Fuzzy Syst.* 2022, 31(4):1254–1266.

[13] Wang J, Wang C, Chen CP, Liu Z, Zhang C. Fast finite-time event-triggered consensus control for uncertain nonlinear multiagent systems with full-state constraints. *IEEE Trans. Circuits Syst. I, Reg. Pap.* 2022, 70(3):1361–1370.

[14] Min H, Xu S, Zhang Z. Adaptive finite-time stabilization of stochastic nonlinear systems subject to full-state constraints and input saturation. *IEEE Trans. Autom. Control* 2020, 66(3):1306–1313.

[15] Yao D, Dou C, Zhao N, Zhang T. Practical fixed-time adaptive consensus control for a class of multi-agent systems with full state constraints and input delay. *Neurocomputing* 2021, 446:156–164.

[16] Hou HQ, Liu YJ, Lan J, Liu L. Adaptive fuzzy fixed time time-varying formation control for heterogeneous multiagent systems with full state constraints. *IEEE Trans. Fuzzy Syst.* 2022, 31(4):1152–1162.

[17] Zhu J, Shen Q, Zhang T, Yi Y. Decentralized finite-time adaptive neural FTC with unknown powers and input constraints. *Inf. Sci.* 2024, 656:119909.

[18] Gong J, Jiang B, Ma Y, Mao Z. Distributed adaptive fault-tolerant formation control for heterogeneous multiagent systems with communication link faults. *IEEE Trans. Aerosp. Electron. Syst.* 2022, 59(2):784–795.

[19] Gong J, Jiang B, Ma Y, Mao Z. Distributed Adaptive Fault-Tolerant Formation–

Containment Control With Prescribed Performance for Heterogeneous Multiagent Systems. *IEEE Trans. Cybern.* 2022, 53(12):7787–7799.

[20] Yu Z, Qu Y, Zhang Y. Distributed fault-tolerant cooperative control for multi-UAVs under actuator fault and input saturation. *IEEE Trans. Control Syst. Technol.* 2018, 27(6):2417–2429.

[21] Van M, Ge SS. Adaptive fuzzy integral sliding-mode control for robust fault-tolerant control of robot manipulators with disturbance observer. *IEEE Trans. Fuzzy Syst.* 2020, 29(5):1284–1296.

[22] Yao L, Wu Y. Robust fault diagnosis and fault-tolerant control for uncertain multiagent systems. *Int. J. Robust Nonlinear Control* 2020, 30(18):8192–8205.

[23] Wang H, Zhou X, Tian Y. Robust adaptive fault-tolerant control using RBF-based neural network for a rigid-flexible robotic system with unknown control direction. *Int. J. Robust Nonlinear Control* 2022, 32(3):1272–1302.

[24] Zhao Y, Zhou M, Xu X, Zhang N. Fault diagnosis of rolling bearings with noise signal based on modified kernel principal component analysis and DC-ResNet. *CAAI Trans. Intell. Technol.* 2023, 8(3):1014–1028.

[25] Qin C, Jin Y, Zhang Z, Yu H, Tao J, *et al.* Anti-noise diesel engine misfire diagnosis using a multi-scale CNN-LSTM neural network with denoising module. *CAAI Trans. Intell. Technol.* 2023, 8(3):963–986.

[26] Yuan C, Zhang Y, Liu Z. A survey on technologies for automatic forest fire monitoring, detection, and fighting using unmanned aerial vehicles and remote sensing techniques. *Can. J. For. Res.* 2015, 45(7):783–792.

[27] Liu C, Jiang B, Zhang K, Ding SX. Hierarchical structure-based fault-tolerant tracking control of multiple 3-DOF laboratory helicopters. *IEEE Trans. Syst. Man Cybern. Syst.* 2021, 52(7):4247–4258.

[28] Yu X, Li P, Zhang Y. The design of fixed-time observer and finite-time fault-tolerant control for hypersonic gliding vehicles. *IEEE Trans. Ind. Electron.* 2017, 65(5):4135–4144.

[29] Kamel MA, Ghamry KA, Zhang Y. Real-time fault-tolerant cooperative control of multiple UAVs-UGVs in the presence of actuator faults. *J. Intell. Robot. Syst.* 2017, 88:469–480.

[30] Yoo SJ, Kim TH. Predesignated fault-tolerant formation tracking quality for networked uncertain nonholonomic mobile robots in the presence of multiple faults. *Automatica* 2017, 77:380–387.

[31] Hosseinzadeh M, Yazdanpanah MJ. Performance enhanced model reference adaptive control through switching non-quadratic Lyapunov functions. *Syst. Control Lett.* 2015, 76:47–55.

[32] Tao G. Model reference adaptive control with L 1+ α tracking. *Int. J. Control* 1996, 64(5):859–870.

[33] Liu YJ, Li J, Tong S, Chen CP. Neural network control-based adaptive learning design for nonlinear systems with full-state constraints. *IEEE Trans. Neural Netw. Learn. Syst.* 2016, 27(7):1562–1571.